Siehe auch: Renewable and Sustainable Energy Reviews, Volume 137, 110646, 2020, https://doi.org/10.1016/j.rser.2020.110646

Pre-Print: doi:10.17170/kobra-202103103481, 2019

Large-scale heat pumps: market potential and barriers, classification and estimation of efficiency

Jesper, M.[1,], Schlosser, F.[2,3], Pag, F.[1], Schmitt, B.[1], Walmsley, T.G.[3], Vajen, K.[1]*

[1] *University of Kassel, Department of Solar- and Systems Engineering, Kurt-Wolters-Str. 3, 34125 Kassel, Germany*
[2] *University of Kassel, Department of Sustainable Products and Processes, Kurt-Wolters-Str. 3, 34125 Kassel, Germany*
[3] *Sustainable Energy & Water Systems Group, School of Engineering, University of Waikato, Hamilton, New Zealand*

Abstract

Heat pumps powered by renewable electricity have a significant potential to become a critical technology to disruptively decarbonize an economy. An essential step towards this goal is the development of an accurate understanding and model of how heat pumps in large-scale implementations perform in terms of economics, energy, and the environment. In this study, the influence of system design and operating conditions on the Coefficient of Performance (COP) of large-scale (> 50 kW_{th}) electric driven mechanical compression heat pumps is reviewed, leading to a methodology to estimate a heat pump's performance depending on the operating conditions. An overview of the potential scale, market size and barriers for large-scale heat pumps with a focus on applications in industry, commerce and district heating systems is given. The review underscores the knowledge gap in the area of large-scale heat pumps including their lack of performance testing standards given the large window of operating conditions as well as meaningful application possibilities. Transferring a significant and reliable dataset to practitioners (e.g. energy-managers and consultants) can close this knowledge gap. Therefore, this study assembles a comprehensive dataset for the system configuration and performance of 33 large-scale heat pumps from 11 different manufacturers and addresses three main objectives: (1) Classifying and evaluating the capabilities of market available heat pumps. (2) Modelling the correlation between the COP and the operating conditions. (3) Developing an economic and ecological evaluation method for a heat pump project. Applying the developed models to accurately assess real-world performance and build a sound business case for large-scale heat pumps has the potential to accelerate the uptake of renewable energy and help improve overall environmental sustainability.

Highlights:

- Summaries the potential and capabilities of market available heat pumps
- Examines the influence of system configuration on heat pump efficiency
- Develops accurate models for estimating the COP depending on operating conditions
- Presents a short-cut method for economic and ecological feasibility assessment

Keywords: heat pump, high temperature, COP, temperature lift, state of technology, feasibility assessment

Word count: 11,163

Nomenclature

a	annuity factor [-]
A	annuity [€/a]
b	price dynamic cash value factor [-]
c_p	isobar heat capacity [kWh/(kg·K)]
c	specific Cost [€/kWh]
C	costs [€]
CHP	combined heat and power
DH	district heating

[*] Corresponding author.
E-mail address: solar@uni-kassel.de

SGB	standard gas boiler
SHP	standard electric driven mechanical compression heat pump
COP	coefficient of performance [-]
CPS	climate protection scenario
E_{el}	consumed electric energy [kWh]
EF	emission factor [g_{CO2}/kWh]
f	effect factor [%]
GHGE	greenhouse gas emissions [g_{CO2}]
GWP	global warming potential [-]
HC	hydrocarbons
HCFO	hydrochlorofluoroolefins
HFC	hydrofluorocarbons
HFO	hydrofluoroolefins
HP	electric driven mechanical compression heat pump
HTHP	high temperature electric driven mechanical compression heat pump
LCOH	levelized cost of heat [€/kWh]
n	number [-]
N	depreciation period
NBT	normal boiling temperature [°C]
p	pressure [bar]
pc/p0	pressure ratio [-]
P_{el}	electric power input [kW]
q	interest-rate factor
Q_{dem}	annual reference energy demand
$Q_{h,use}$	usable thermal energy [kWh]
$\dot{Q}_{h,use}$	usable heat output [kW]
R^2	coefficient of determination
R717	ammonia
SCOP	seasonal coefficient of performance [-]
SG	safety group classification [-]
t	temperature [°C], time [h]
T	temperature [K]
VHC	volumetric heating capacity [kJ/m³]
VHTHP	very high temperature electric driven mechanical compression heat pump

Greek symbols

γ	heat capacity ratio [-]
ΔT	temperature difference [K]
$\varepsilon_{isentropic}$	isentropic compressor efficiency [-]
η_{2nd}	2nd law efficiency [-]
μ	expected value
ρ	density [kg/m³]
σ	standard deviation
Σ	sum

Subscripts

0	evaporation
c	condensation
cap	capital-related
Carnot	Carnot
crit	critical
dem	demand-related
dr	driving gradient
e	equivalent
fu	fuel
h	heat sink
in	inlet
l	heat source
lift	lift

m	maintenance
max	maximum
ng	natural gas
NBT	normal boiling temperature
o	outlet
oh	operation hours
op	operation-related
ref	reference system
th	thermal

1. Introduction

Large-scale heat pumps (> 50 kW_{th}), especially for waste heat recovery and powered by renewable electricity, are an important and economically promising technology for the disruptive decarbonisation of low temperature heat demand of industry, commerce, district heating (DH) systems and large communal or residential buildings. Excess heat is broadly available in industrial plants, and a substantial proportion could be recovered and upgraded to displace conventional fossil heat generation and to reduce greenhouse gas emissions (GHGE). In comparison to environmental heat sources (ambient air, near-surface geothermal energy, lake, river or seawater), the temperature of many excess heat sources is relatively high, which results in an increased heat pump efficiency, reduced operating costs, and improved competitiveness to conventional fossil fuel-driven heat generators. Sequentially, several studies stated the high potential of excess heat recovery using heat pumps to supply different industries or DH systems (see section 1.1). The state of research regarding the technical potential of heat pumps in industry and DH, market overview and barriers as well as the efficiency assessment of heat pumps is reviewed in the following sections (Sections 1.1 to 1.4).

1.1 Technical potential of large-scale heat pumps in industry and DH

Due to the oil crises in the 1970s, there was a strong emergence of research work and scientific publications in the field of large-scale heat pumps in the following years [1]. An example of this is Eder and Moser [2] describing suitable applications of heat pumps in industrial plants for drying, evaporation or distillation. They also defined selection criteria for heat pumps and described economic application possibilities. In the late 1980s, 1990s and early 2000s, the general interest in this topic weakened again. Due to intensified efforts to decarbonize heat supply, the attention to large-scale heat pumps is increasing again since the late 2000s. This is confirmed by many published case studies, of which some are presented below:

The HPTCJ-Institute of Japan investigated the heat recovery potential in the food and beverages industry in China, USA and nine European Countries. It was found that the usage of heat pumps for heat recovery could save up to 105 TWh/y of primary energy in total, which equals 15 % of the entire primary energy demand in this industry in the investigated countries [3]. Almost the same relative technical potential was indicated in another study that investigated the French food and beverage industry. This study names an absolute technical potential of 15 TWh/a of heat recovery using heat pumps, which also equals 15 % of the industries total energy consumption [4]. Dupont and Sapora [5] compared the low temperature excess heat availability (35 – 70 °C) to the heat demand which could be supplied by heat pumps (60 - 140 °C) for seven further industries in addition to the food and beverage industry. One of the main findings is that the potential excess heat utilization with heat pumps in food and beverage, dairy, transport equipment, cement, lime and plaster industries exceeds the low temperature heat demand by 4 – 31 %.

Besides the internal use of excess heat in industrial or commercial companies, the usage of excess heat to supply external consumers via DH is seen as a promising option to increase overall efficiency and to reduce GHGE [6]. Additionally, the role played by large-scale heat pumps in DH utilizing environmental or sewage water heat is especially important. “Heat Roadmap Europe 4”, a comprehensive study by Paardekooper et al. [7] on the economic and ecological share of DH, predicts it will cover around half of Europe’s heating market in 2050. With a share of 25 % of the whole DH-demand, large-scale heat pumps utilizing environmental or sewage water heat are seen as the second most important heat generator following biomass or natural gas-fueled combined heat and power (CHP). This is the fact, although industrial excess heat is not considered as a heat source for heat pumps. But similar to further studies like Reckzügel et al.[8], which also avoid the high complexity of determining the low temperature industrial excess heat availability and modelling the resulting potential due to the utilization with the help of heat pumps, it is stated that this could additionally increase the importance of large-scale heat pumps in DH significantly. Reasons for this are the high availability of low temperature excess heat sources in urban areas and the usually higher temperatures of excess heat sources in comparison to environmental or sewage water heat.

1.2 Market overview and barriers

In contrast to the high technical potential of large-scale heat pumps, the overall market penetration is extremely low. This is especially true for heat pumps in industry. Wolf [9] lists 38 realized heat pumps in European, five in Japanese and one in Canadian industry. Laue et al. [10] describe 115 large-scale heat pump applications in Austria, Canada, Denmark, Germany, Japan, Korea, the Netherlands and Switzerland of which some are also covered by Wolf [9]. Most of these heat pumps are internally utilizing waste heat in Industry, but some supply into DH. Still, the overall share of heat that is provided by heat pumps in the European industry is negligible [9,11].

David et al. [6] found 149 large-scale heat pumps (> 1 MW_{th}) operated in DH, accounting for a total output capacity of 1580 MW_{th}. The scope of that work included the EU-28, Norway and Switzerland but large DH-heat pumps have only been identified in 11 of those countries. With approximately 1 GW_{th}, most of the installed capacity is located in Sweden and was built in the 1980s. A driver for this was a legal framework that promoted power to heat because of a temporary surplus in electricity produced by newly-built nuclear power plants. Following the all-time high of installed heat pump-capacity in the 1980s, the newly installed capacity decreased in the following decade. Since the turn of the millennium, the yearly installed capacity is increasing again and mainly located in Finland (155 MW_{th}), Italy (37 MW_{th}), France (23 MW_{th}) and Denmark (20MW_{th}). The temporal development of installed heat capacity is similar to the development of research work and scientific publications described in Section 1.1. But even with 149 realized projects in European DH, the potential in this area is far from being reached.

There are several barriers for a wider uptake of large-scale heat pumps. The economic conditions for heat pumps are often unfavorable, which is particularly visible in the high ratio of electricity to gas (or oil) costs in many countries. In a European comparison, this ratio is particularly high in Germany. One reason for this is the unequal burden of electricity in comparison to other final energy carriers caused by a levy for the cost of renewable energy integration. This is largely responsible for the strong reduction of the potential economic share (3.4 %) in comparison to the potential technical share (23.3 %) of useful heat demand covered by heat pumps in German industry [9]. For DH-heat pumps, this is practically made clear by the fact that none of the 149 listed heat pumps in David et al. is located in Germany. Wolf [9] mentions more than 60 heat pumps in European DH from which only two are located in Germany. Further reported economic barriers are relatively high payback periods (> 3 years) and cost-intensive integration into existing processes because of the need to customize the design [12–14]. Besides the economic barriers, there are also technical barriers reported. Here, the limitation of the heat sink temperature and the availability of refrigerants with a low global warming potential (GWP) are often mentioned [12–14]. At the same time, the technical progress and the resulting progressive debilitation of the technical barriers are pointed out [9,14].

The third important barrier is about the missing knowledge on the topic of excess heat and heat pumps [12–14]. On the one hand, the quantity of heat demand and emitted excess heat is mostly unknown in companies. In a survey of 7,288 German companies 86 % were not able to estimate their amount of excess heat On the other hand, the knowledge of technical options for excess heat utilization is low. 53 % of the surveyed companies rate their knowledge on this topic as good to very good but 50 % of the companies are still interested in more information. This goes along with the fact that for projecting a heat pump for excess heat utilization the combined knowledge on the capabilities of large-scale heat pumps and the process itself is needed; however, energy-managers, -consultants and decision-makers rarely have this information [12,14]. Additionally, there is a lack of guidelines and standards, pilot and demonstration systems and training events on the topic of excess heat utilization and large-scale heat pumps.

1.3 Measuring and publishing of information on heat pump efficiency

One basic parameter to describe the efficiency of a heat pump is the coefficient of performance (COP). The COP compares the usable heat output to the power input at stationary conditions (see Eq. 1-1). For electric driven mechanical compression heat pumps (HP), the motive force is electricity and, according to the European Standard EN 14511-1 [15], it includes the compressor and all auxiliary facilities like pumps and the control system.

$$COP = \dot{Q}_{h,use}/P_{el} = \left[\left(t_{h,out} - t_{h,in}\right) \cdot \dot{V}_h \cdot \rho_h \cdot c_{p,h}\right]/P_{el} \qquad \text{Eq. 1-1}$$

For the measurement and publishing of the COP characteristics, most manufacturers proceed according to the European Standard EN 14511, which is divided into four parts [15–18]. This standard defines parameters and respective test-conditions and -methods for technical data sheets of HPs for space heating and -cooling and process cooling. Since there is no standard available for different applications like process heating or DH, even the technical information on most HPs, which are dedicated for applications not covered by the EN 14511, are still tested and published on the basis to this standard with minor variations. The defined parameters include the heat output and COP at the nominal operating point which is defined by the inlet and outlet temperatures at the evaporator and condenser at maximum electric power intake (Figure 1). The flow rates of the heat source and sink at the nominal operating point are a result of the nominal temperatures and the respective heating and cooling capacity.

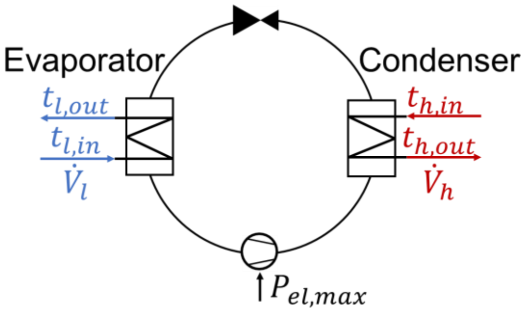

Figure 1: Schematic of nominal test conditions of a HP according to EU Standard EN 14511 [15–18].

The prescribed heat carrier temperatures at the evaporator depend on the heat source temperature (see Table 1). To meet the requirements of different space heating systems, the condenser temperatures must be chosen out of four different options.

Table 1: Nominal temperatures for water/water and brine/water HPs according to EN 14511 [17].

Medium of heat source	$t_{l,in}$ $in\ °C$	$t_{l,out}$ $in\ °C$	Temperature of heat sink	$t_{h,in}$ $in\ °C$	$t_{h,out}$ $in\ °C$
Water	10	7	Low	30	35
Brine	0	-3	Intermediate	40	45
			Medium	47	55
			High	55	65

The seasonal coefficient of performance (SCOP) puts the seasonal (usually yearly) heat gain in proportion to the electric energy effort (see Eq. 1-2) and is the crucial parameter to evaluate the efficiency of a projected heat pump and sets the basis for economic and ecologic evaluation. To calculate the SCOP, detailed knowledge of the correlation between the COP and all operating conditions occurring during a specific season must be known.

$$SCOP = Q_{h,use}/E_{el} \qquad \text{Eq. 1-2}$$

To calculate the SCOP based on the COP-characteristics as well as on the load and temperature profiles, various methods such as simulation- or spreadsheet-software are used in practice. For more standardized applications like space heating or domestic hot water supply, there are also simplifying methods like the VDI 4650 [19] available, which uses correction factors including assumptions on varying load- and temperature-profiles. Since the temperatures of excess heat sources and process heat sinks are in many cases not influenced by the outside temperature and any fluctuations in load profiles can be smoothed by thermal energy storages, especially industrial HPs are often operated under almost constant conditions [20]. In these cases, the SCOP is almost identical to the COP under the respective operating conditions.

Since the load and temperature profiles can vary strongly from application to application, heat pump manufacturers can not publish SCOP values which are representative for a broad range of applications. As a result, it is reasonable to estimate the SCOP based on COP characteristics published by the manufacturers and the load and temperature profiles for each application individually within the feasibility assessment.

1.4 Objective

According to the EU Standard EN 14511, technical data sheets which are available in public (e.g. on manufacturers homepage) usually only contain information on the COP for one or a few nominal operating points.

Information on the COP over an entire operating range is in most cases only available for a limited number of parties, like engineering offices or plant manufacturers, that have business relations to heat pump manufacturers. For many applications, the estimation of the COP (or SCOP) and sequentially the undertaking of a feasibility study is not possible for important practitioners like energy-managers or -consultants. Additionally, most actors in the field of heat pump surveying have information on the capabilities of heat pumps limited to one or two manufacturers. Knowledge of the capabilities of the heat pumps over the whole market is rare.

The Guideline 4646 by the Association of German Engineers (VDI), which is currently under development, aims to close this knowledge gap on the requirements, system design and capabilities of large-scale heat pumps. It is intended to simplify the preliminary planning for applications in industry, municipal facilities (e.g. swimming pools), DH and large residential and non-residential buildings. The overall goal is to enable a broad audience to do a quick feasibility assessment including an ecological and economic evaluation. The fact that no satisfactory existing feasibility assessment method could be identified within the elaboration of the VDI 4646 was the decisive point that initiated the development of a new method, which is presented in this work. As a result, the three main objectives of the study are:

1. Classifying and evaluating the capabilities of market available HPs (see Section 2). For this purpose, a comprehensive database representing market available HP technologies was assembled and is analyzed. In that course, the market available HPs are categorized depending on their COP-characteristics.
2. Modelling the correlation between the COP and the operating conditions of the categorized HPs in a regression analysis (see Section 4). Therefore, new approaches are developed, which are capable of higher accuracy than the typical approach based on the Carnot-COP and a constant 2nd law efficiency (η_{2nd}).
3. Developing an economic and ecological evaluation method for a HP project based on the derived mathematical models for estimating the COP (see Section 5). For that purpose, nomograms are developed comparing the levelized cost of heat (LCOH) and the GHGE resulting from the operation of a HP and a standard gas boiler (SGB) and depending on the operating conditions.

2. Classification of market-available heat pumps and their capabilities

The market for large-scale heat pumps is complex. The system configuration of the offered heat pumps varies strongly to meet the requirements of a broad range of applications in the best possible way. To understand the characteristics and capabilities of the resulting diversity of system configurations would exceed the scope of this work. A standard system configuration was defined which is intended to represent a greater part of the market for large-scale heat pumps and the state of technology:

- Electric driven single-stage compression
- Subcritical closed-loop process
- Thermal output: $\geq 50\ kW_{th}$
- Heat source: brine and water
- Heat sink: water
- Compressor: reciprocating piston, screw, scroll and turbo
  (no restrictions concerning open, semi-hermetic or hermetically sealed)
- Refrigerant: azeotrope or quasi azeotrope with negligible temperature glide,
  synthetic-organic or natural
- No restrictions on further system design (internal heat exchanger, economizer etc.)

Ten manufacturers have contributed information to this study. Since it was agreed with the manufacturers that the provided data will only be published anonymously, no names or type designations will be published in this work. For further evaluation, the gathered information was transferred to a common database. Single operating points over the whole operating range of each HP were extracted with a minimum step size of 5 K for $t_{l,in}$ and $t_{h,out}$. Most manufacturers offer different sizes of the same series. For most cases, the COP characteristics of the different sizes of one series are similar. As a result, only one HP size in the middle of the range of each series was added to the database. An exemption from this was made for one series. In this series, which is offered with a nominal thermal output of 0.1 MW_{th} to 0.8 MW_{th}, major (> 10 %) variations in COP for the same operating temperatures occur between the different sizes. In this case, one HP in the lower and one in the higher thermal output range of this series was considered. In total, 425 operating points of 29 HPs are included in the database. The nominal heat output of these HPs ranges from 50 kW_{th} to 1.5 MW_{th}, with focus on the range up to 0.4 MW_{th}. The absolute thermal output considering all covered operating points ranges between 25 kW_{th} and 1.8 MW_{th}. Additionally, 8 operating points of four HPs (Kobe Steel Kobelco SGH 120, Combitherm HWW R245fa, Ochsner IWWDS ER3b and Ochsner IWWDS ER3c4), which fit the defined standard configuration, are taken from Arpagaus et al. [12].

Pre-Print: doi:10.17170/kobra-202103103481

2.1 *Operating temperatures*

The heat source and sink temperatures of the gathered operating points are illustrated in Figure 2. The clear focus lies in the conventional operating range ($t_{l,in}$ < 40 °C and $t_{h,out}$ < 80 °C), 76 operating points are located in the high temperature range (40 °C≤ $t_{l,in}$ < 60 °C and/or 80 °C ≤$t_{h,out}$ < 100 °C) and 37 in the very high temperature range ($t_{l,in}$ ≥ 60 °C and/or $t_{h,out}$ ≥ 100 °C).

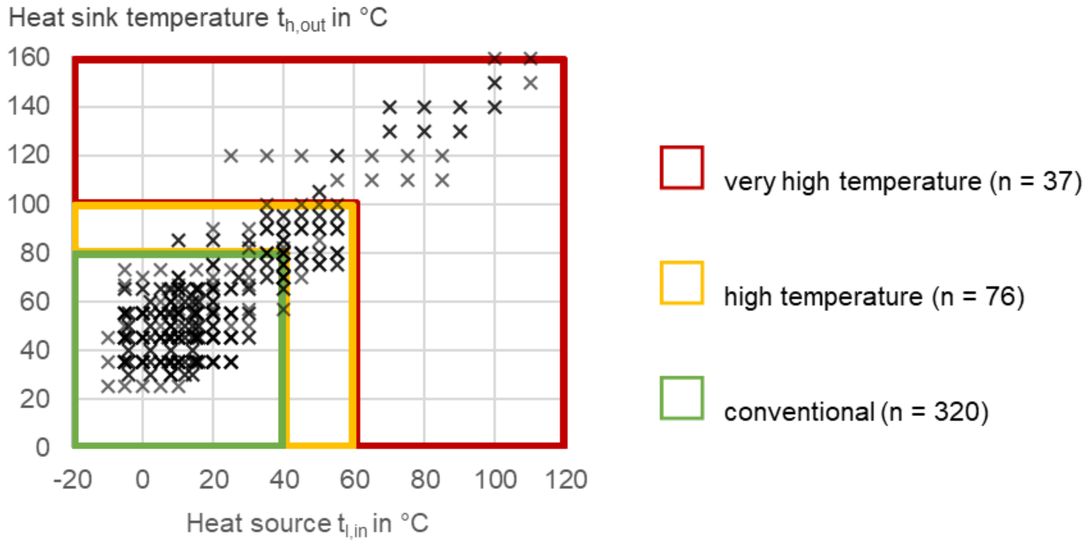

Figure 2: Classification of the operating point database. The classification scheme is adapted from Arpagaus et al. [12], which was based on [14,21–24].

Table 2 illustrates the classification of the heat pumps covered in this work. 18 out of 33 HPs only operate in the conventional source-sink window. An additional seven HPs sit outside the conventional and within the high temperature operating range. In total, 90 % of the gathered operating points sum under the classifications of standard (SHP) and high temperature HPs (HTHP). Despite the relatively high number of HPs that operate in the high and very high temperature ranges (8 out of 33 HPs), less than 10 % of the operating points can be allocated to very high temperature heat pumps (VHTHP).

Table 2: Classification of heat pumps

Heat pump class	Temperature range of operation	Heat pumps	Operating points
VHTHP	Very high	7	8 %
	High and very high	1	2 %
HTHP	High	0	0 %
	Conventional and high	7	26 %
SHP	Conventional	18	64 %

2.2 *Refrigerants*

The manufacturers provided information on heat pumps using nine different refrigerants (see Table 3). With 21 out of 33 HPs and 76 % of the operating points, hydrofluorocarbons (HFC) is the most dominant refrigerant class. Hydrofluoroolefins (HFO) and hydrochlorofluoroolefins (HCFO) have usually a lower GWP and a similarly advantageous safety classification in comparison to alternative HFC. However, since the manufacturers only provided information on four HFO-HPs, one HCFO-HP and two HPs using R513A (HFO/HFC-mixture), it can be concluded that the usage of these refrigerant-classes remains scarce in 2019. R717 (ammonia) is the only natural refrigerant covered in this work. Based on manufacturers data, 18 operating points from five R717-HPs are included in the database. Due to the high evaporation enthalpy of R717, this refrigerant is particularly suitable for high capacities with a compact design and low refrigerant quantities. However, its toxicity and flammability require special safety measures, which favor use outside residential buildings in large-scale industrial HPs where tight controls can be implemented. All HP data points covered in this work with a nominal thermal output of more than 0.8 MW use R717.

The usage of alternative natural refrigerants in large-scale heat pumps with a low GWP and a favorable safety classification like R718 (water) or R744 (carbon dioxide) is still not state-of-the-art technology in 2019 (R718) or not covered by this work due to its transcritical operation (R744). Hydrocarbons (HC) like R600 (n-butane) or R601 (pentane) have a low GWP but are highly flammable. EN 378-1 [25] limits the filling capacity of these HPs to a maximum of 2.5 kg, making HC inappropriate for large-scale HPs and further explains why no large-scale commercial HPs use these refrigerants.

Table 3: Refrigerants used by the heat pumps in the database.

	R1336mzz(Z)	R1233zd(E)	R1336mzz(E)	R245fa	R1234ze(E)	R717	R134a	R513A	R410A
Class	HFO	HCFO	HFO	HFC	HFO	natural	HFC	HFO/ HFC*3	HFC
Heat pumps	1	1	1	6	2	5	9	2	6
Operating points	3 %	2 %	2 %	12 %	9 %	4 %	34 %	5 %	30 %
GWP*1	2	1	18	858	< 1	0	1300	631	2088
SG*2	A1	A1	A1	B1	A2L	B2L	A1	A1	A1

*1 GWP for a 100-year time horizon [12,26]
*2 Safety group classification (SG) according to [25,27] and taken from [12,26]
*3 R513A is a mixture of R1234yf (56 %, HFO) and R134a (44 %, HFC) [26]

2.2.1 Temperature operating range

Figure 3 illustrates the operating temperature range and the maximum temperature lift (ΔT_{lift}) of the nine used refrigerants. For R513A, R245fa and R1336mzz(E), the operating range and ΔT_{lift} are equal. For the rest of the refrigerants, ΔT_{lift} is smaller than the operating range, probably caused by limitations of the compressor. The maximum ΔT_{lift} lies for all but one HP between 60 and 78 K. The HP "Kobe Steel Kobelco SGH 120" [12] is the only exception. In a single-stage compression using R245fa, this heat pump reaches a maximum temperature lift of 95 K by transferring excess heat from 25 °C to 120 °C.

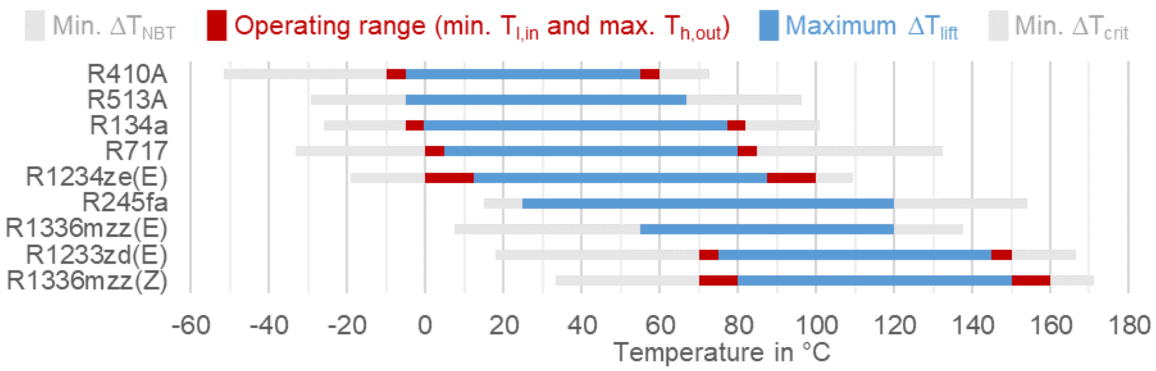

Figure 3: Normal boiling temperature at 1.013 bar (NBT, left end of grey bar) [12,26], minimum $t_{l,in}$ (left end of red/blue bar), maximum temperature lift (ΔT_{lift}, blue bar), maximum $t_{h,out}$ and critical temperature (t_{crit}, right end of grey bar) [12,26] of the nine refrigerants.

For subcritical HPs, which are the scope of this work, the maximum $t_{h,out}$ is limited by t_{crit}. Usually, a heat pump operation below ambient pressure is avoided [28]. Therefore, the lower operating boundary is given through the normal boiling temperature at 1.013 bar. In Figure 3, the difference between the real operating range and NBT or t_{crit} is exemplified. For R410A, R134a, R1234ze(E), R1336mzz(E), R1233zd(E) and R1336mzz(Z), the difference of t_{crit} and $t_{h,out}$ (ΔT_{crit}) is 9 to 19 K. When the driving temperature gradient of the condenser ($T_{dr,h}$) and a subcooling is considered, the minimum difference to this upper operating boundary is almost exhausted for these refrigerants. This is especially true when considering that the COP is particularly low at condensation temperatures (t_c) close to t_{crit} (Figure 4 (a)) because of the narrowing two-phase area.

ΔT_{crit} is relatively high for R717 (47 K), R245fa (34 K) and R513A (30 K). This suggests the conclusion that higher $t_{h,out}$ could be reached, which could extend the operating range of the HPs using these refrigerants. For R513A, this seems to be true but, for R717 and R245fa, there are reasons to explain the relatively high ΔT_{crit}:

- R717: The critical pressure is 113 bar [29]. Currently, the maximum achievable pressure for commercial R717-HTHPs is 76 bar [12]. The maximum $t_{h,out}$ recorded in the collected data is 85 °C. If a ΔT_{crit} of 10 K is assumed, this equals a condensation pressure (p_c) of 57 bar [29]. By limiting the maximum pressure below what is technically possible, costs can be saved because the construction complexity is reduced.

- R245fa: In a simulation study, Arpagaus et al. [12] find that R245fa reaches particularly low COP for t_c above of 100 °C. If t_c is further increased towards t_{crit} (154 °C), the COP of R245fa deteriorates even more compared to nine different refrigerants including R1336mzz(Z), R1233zd(E) and R1234ze(Z). To avoid an unnecessarily low COP, R245fa is therefore not used to reach $t_{h,out}$ above of 120 °C.

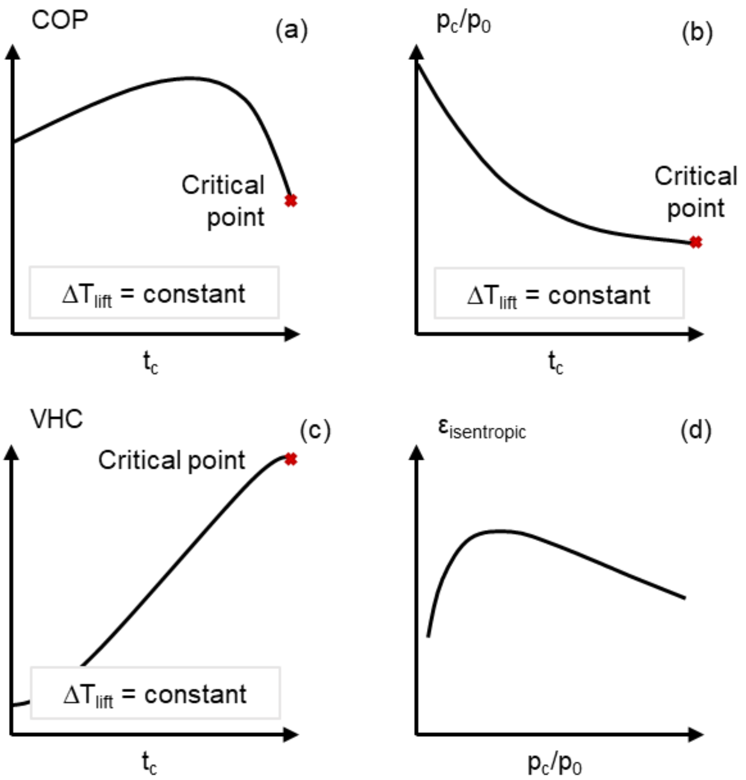

Figure 4: Qualitative development of the COP (a), the pressure ratio (p_c/p_0) (b), the volumetric heating capacity (VHC) (c), all for a range of condensation temperatures (t_c) (adapted from Arpagaus et al. [12]), and the isentropic compressor efficiency ($\varepsilon_{isentropic}$) depending on p_c/p_0 (d) (adapted from Maurer [28]).

The minimum difference between $t_{h,in}$ and NBT (ΔT_{NBT}) is for all refrigerants, except R245fa, to be at least 19 K. This is considerably more than what is necessary to ensure sufficient superheating and to consider the driving temperature gradient of the evaporator ($T_{dr,l}$). Among others, there are three practical reasons to explain why ΔT_{NBT} is relatively high for most refrigerants and why the resulting limitation of the operating range is acceptable:

- The pressure ratio (p_c/p_0) is increasing when t_c is decreasing and ΔT_{lift} is constant (see Figure 4 (b)). A p_c/p_0 in the upper compressor operating range results in a relatively low isentropic compressor efficiency ($\varepsilon_{isentropic}$) (see Figure 4 (d)) and a low COP. The relatively low COP for t_c in the lower operating range is also visible in Figure 4 (a). Additionally, the maximum pressure ratio is technically limited. For instance, the maximum p_c/p_0 of reciprocating piston and screw compressors usually lies between 10 and 20 and the optimum efficiency is around 5 [28].

- VHC is decreasing when t_c is approaching the NBT and ΔT_{lift} is constant (see Figure 4 (c)). This is opposed to the fact that a higher VHC is advantageous for reciprocating piston, screw and scroll compressors because it leads to a smaller size at a given capacity and also to reduced investment costs [12].

- For some refrigerants, the two-phase area in a log(p)-h-diagram is strongly overhanging. As a result, an relatively increased superheating before suction is required to ensure a dry compression. For instance, Arpagaus et al. [12] found that, for R1336mzzz(Z), superheat of 21 K before suction is needed to ensure superheat of 5 K after compression. In contrast, for other refrigerants like R245fa a superheat obfore suction of 5 K is sufficient.

ΔT_{NBT} is by far the lowest for R245fa (10 K). This can be explained by the fact that that the COP-t_c curve for R245fa is decreasing only slightly when t_c approaches NBT [12]. As a result, the operation of R245fa close to the NBT is advantageous.

2.2.2 *Flow and return temperatures*

Regarding the difference between flow and return temperature of the heat-sink and –source, most HPs using HFC, HFO and HCFO are operated following EN 14511-2 [17] (see Figure 5 (a), see also Section 1.3). Almost half of the operating points of the HPs using these refrigerants are stated with a spread between $t_{l,in}$ and $t_{l,out}$ (ΔT_l) of 3 K, which is mandatory for efficiency measurements at the respective nominal operation point. The spread between $t_{h,in}$ and $t_{h,out}$ (ΔT_h) matches for 82 % of the operating points the nominal spread of 5, 8 or 10 K. For the measurement of operating points which differ from the nominal ones, the EN 14511-2 also allows varying spreads if the flow rates are kept at the nominal values. This explains the minor differences resulting from the nominal spreads.

Figure 5 (b) illustrates the spreads of HPs using the non-organic natural refrigerant R717. In contrast to the synthetic-organic refrigerants covered in this work, ΔT_l and particularly ΔT_h differ significantly from the nominal spreads mandated by the EN 14511-2 [17]. An explanation for this is the relatively high heat capacity ratio (γ) of R717 [29]. As a result, R717 reaches significantly higher temperatures after compression in comparison to the organic refrigerants covered in this work. For instance, based on a comparison, R717 reaches 138 °C whilst R134a stays at 42 °C after compression (theoretical dry process, no subcooling after condensation, no superheating after evaporation, t_0 = -30 °C and t_c = 30 °C) [28]. By operating R717-HPs with a high ΔT_h, the high temperature after compression can be utilized for efficiency gains. Additionally, a high spread can also be utilized for subcooling after condensation.

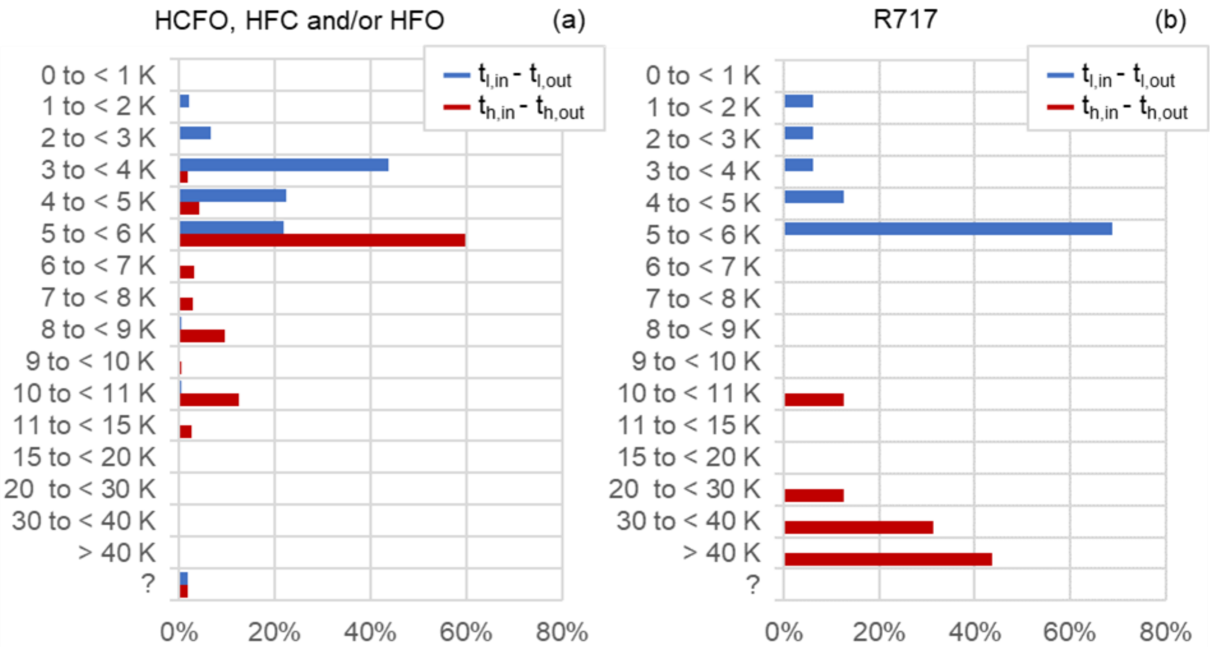

Figure 5: Difference between flow and return temperature of heat-sink and -source according to the surveyed refrigerants.

2.3 Compressor type

The manufacturers provided information on HPs using reciprocating piston, screw and scroll compressors. The distribution of these compressor types is almost balanced among the 33 HPs covered in this work (see Table 4). Regarding the operating points, scroll compressors are more represented than reciprocating piston or screw compressors.

Table 4: Compressor types of heat pumps in the database.

	Reciprocating Piston	Screw	Scroll
Heat pumps	12	11	9
Operating points	29 %	26 %	45 %

Figure 6 illustrates the operating range and maximum ΔT_{lift} of the covered compressor types. The scroll compressors are mainly used in smaller HPs with a nominal heat output between 50 and 170 kW_{th}. The maximum ΔT_{lift} (70 K) and maximum $t_{h,out}$ (82 °C) are the lowest among the three covered compressor types but are sufficient for the intended utilization of environmental heat (near-surface geothermal energy, lake, river or seawater) in large residential buildings or small companies.

When considering only organic refrigerants, HPs using screw compressors are covering the largest nominal thermal output range (0.2 – 0.8 MW_{th}) and are designed for versatile applications with heat sink temperatures up to 120 °C. Screw compressors manage the highest single-stage ΔT_{lift} (95 K) among the covered HPs. Reciprocating piston compressors are used in HPs with organic refrigerants with a nominal thermal capacity ranging from 50 kW_{th} to 0.4 MW_{th}. The HPs using this compressor type are reaching the highest heat sink temperatures (160 °C) and medium ΔT_{lift} (78 K). Both, screw and reciprocating compressors are employed in R717-HPs to reach heat outputs of more than 1 MW.

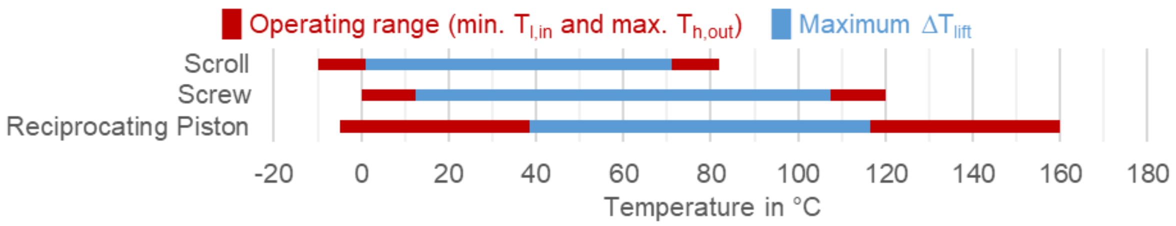

Figure 6: Minimum $t_{l,in}$ (left end of the red bar), maximum ΔT_{lift} (blue bar) and maximum $t_{h,out}$ (right end of the red bar) of the three compressor types.

2.4 COP

Figure 7 visualizes the dependency of the COP on ΔT_{lift} for three different HP-categories which reveal clear differences between the indicated COP curves. These categories were derived based on variances in refrigerants, plant sizes, operation and data availability described in the previous sections and summarized below. Due to the clear differences, these categories will be considered separately in the further course of this work.

- **SHPs & HTHPs with HFC and/or HFO:**
  A wide range of HPs is offered in various sizes with heating supply up to 0.8 MW_{th} and $t_{h,out}$ up to 100°C by different manufacturers. These HPs are often produced in product series and are available from standard stock. Due to the larger quantities sold by these HPs, manufacturers often prepare detailed information such as planning manuals including detailed COP characteristics covering the entire operating range. More than half (20 out of 33 HPs) of HPs and 86 % of the operating point fit into this category. Additionally, the operation of HPs in this category is strongly oriented to the EN14511 (see Section 2.2.2) and the distribution of nominal HP-sizes is reasonably balanced over the whole range (50 kW_{th} to 0.8 MW_{th}) but has a focus to the lower and middle sizes up to 0.4 MW_{th}. The homogeneity of this class is also reflected in the efficiency which is illustrated in Figure 7. There is a clear correlation between COP and ΔT_{lift} with a small range of variation and no obvious outliers. This category represents the state of technology and the largest part of the market for large-scale HPs.
- **VHTHPs with HCFO, HFC or HFO:**

The range of VHTHPs offered is still relatively small with rarely established stock-standard solutions by the manufacturers. Because manufacturers usually provision these HPs individually, they do not prepare comprehensive planning manuals for resellers or plant engineers. As a result, the manufacturers only provided information on five VHTHPs. Additionally, the database was complemented by three VHTHPs from the literature [12]. Eventually, 10 % of the operating points could be accumulated in this category. Although the operation is also oriented to the EN 14511 (see Section 2.2.2) and the offered sizes, used refrigerants and compressors types are similar to the category listed above, the COP of VHTHPs is higher for ΔT_{lift} in the upper range (see Figure 7).

- **SHPs & HTHPs with R717:**
  The properties of R717 differ from the organic refrigerants covered in this work (see Section 2.2). R717 is used in particularly large-scale HPs which are operated with significantly higher ΔT_h. Additionally, the COP of the R717 operating points is noticeable above the remaining HPs (see Figure 7). Whether this is caused through differences in system design, operation, size or by another reason cannot be answered based on the present data. Similar to the case of VHTHPs and due to the large-scale, these HPs are usually built to meet an individual specification. No implementation manuals are available and only 4 % of the operating points belong to this category.

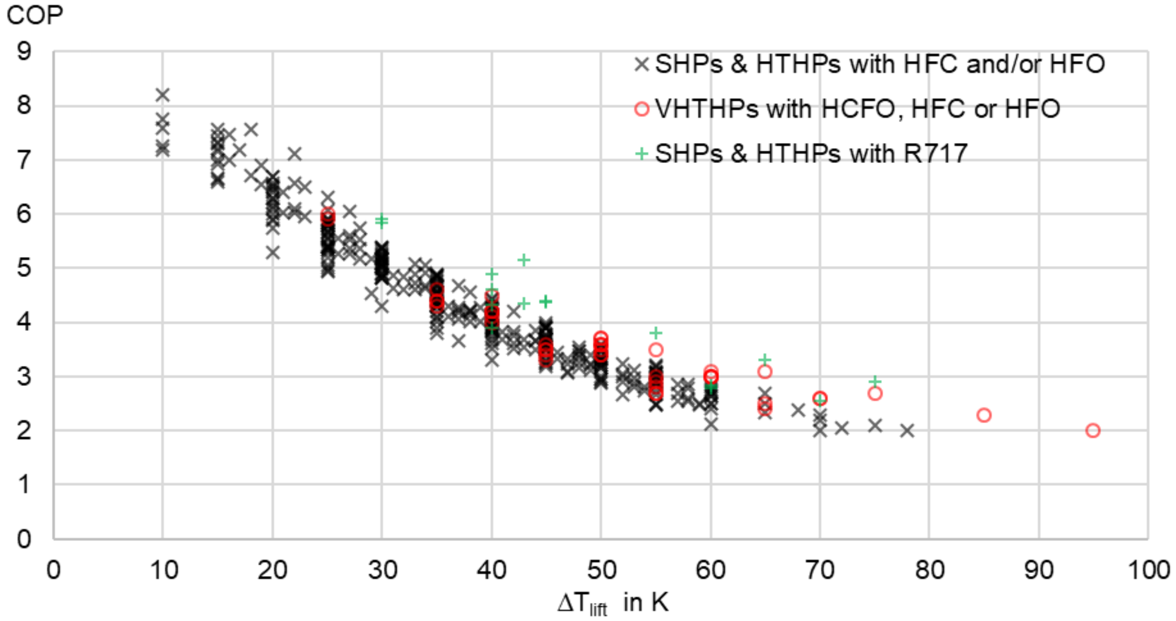

Figure 7: COP depending on ΔT_{lift} for three different HP-categories.

The system configuration of the HPs within the three identified categories is still versatile. The HPs are partly equipped with internal heat exchangers, economizers, different refrigerants or compressor types. Therefore, the following sections examine whether a further subdivision into subcategories within three main categories is reasonable. This is exemplified by the category SHP & HTHP with HFC and/or HFO.

2.4.1.1 Refrigerant

In total, five different organic refrigerants (Figure 8) and three different compressor types (Figure 9) are used. Among the five refrigerants, the COP of R513A and R1234ze(E) is particularly low for small and medium ΔT_{lift} while R410A and R134a are more advantageous in this range. In the upper operating range, this pattern is not observed as no refrigerant shows a clear advantage. The COP of R245fa is for small ΔT_{lift} relatively low but is the highest for 30 K $\leq \Delta T_{lift} \leq$ 60 K.

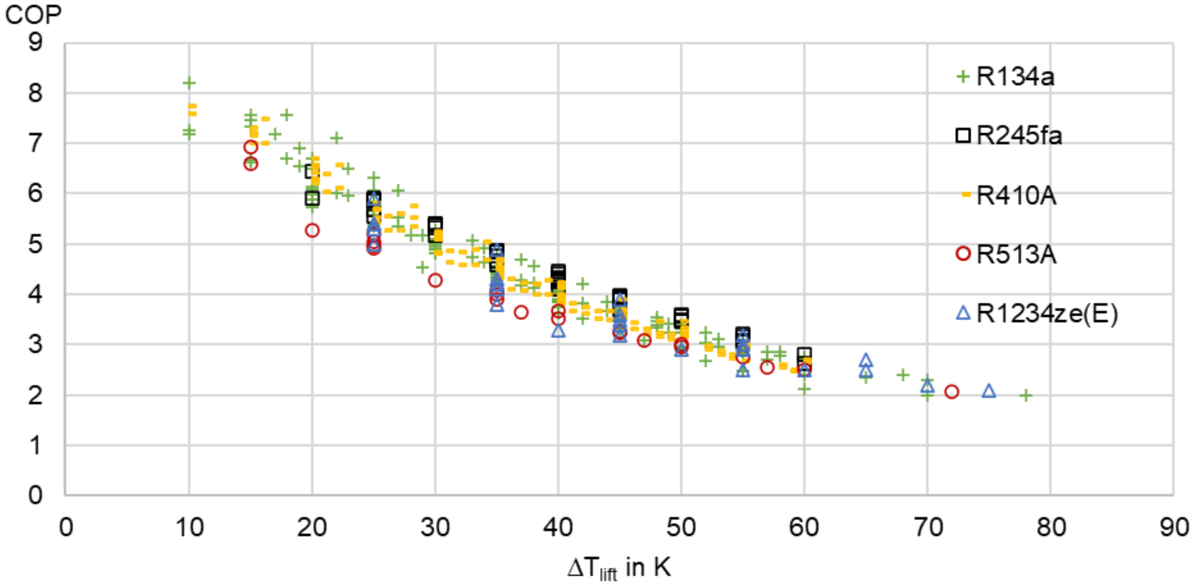

Figure 8: COP depending on ΔT_{lift} for SHPs & HTHPs, highlighting the refrigerants

2.4.1.2 Compressor type

In general, differences of the efficiency between the various compressor types are marginal. Still, the COP of HPs using screw compressors tends for the whole operating range to be slightly higher than the COP of scroll-HPs. HPs using reciprocating piston compressors show small disadvantages for low ΔT_{lift} and small advantages for ΔT_{lift} in the higher operating range. Nevertheless, all three types are overlapping and no clear advantage of one type is recognizable.

It can be summarized that there are differences between refrigerants and compressors regarding the COP but, in most cases, these differences exist for a few operational conditions and are not applicable for the whole operating range. The same belongs to further differences in system design. For instance, some HPs are equipped with internal heat exchangers or economizers but no systematic differences concerning the COP are discernible. Therefore, no further categorization by system configuration is made and the scope of the mathematical models developed in Section 4 covers the three HP-categories defined in Section 2.4.

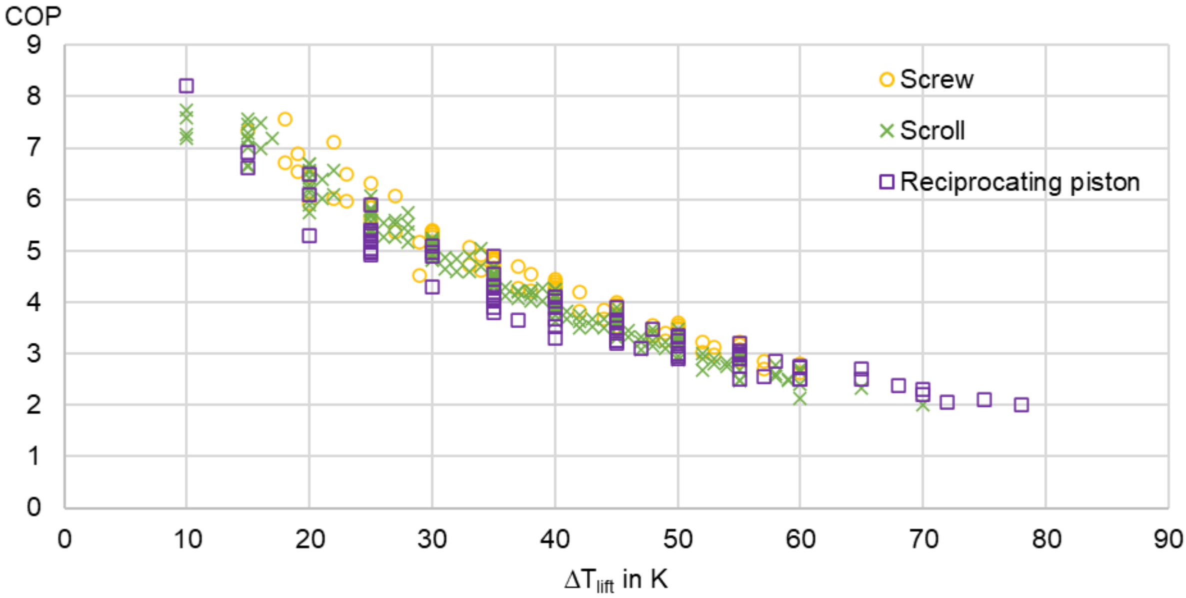

Figure 9: COP depending on ΔT_{lift} for SHPs & HTHPs, highlighting the compressor type

3. Methodology

In Section 2, the database, which is the base of this work, was presented and analyzed. In the further course of this work, the categorized database is used to mathematically model the correlation between the operating conditions of HPs and the COP. These models are used to derive a methodology for a quick feasibility assessment including economic and ecological evaluation. The methodology used for these purposes is presented below.

3.1 Regression analysis

Sections 4.1.1 to 4.1.3 present a regression analysis using the method of the least-squares approximation. Several theoretical, semi-empirical and empirical approaches to estimate the COP for the HP-category SHPs & HTHPs with HFC and/or HFO are derived. This approximation aims to reduce the residuals (deviations) between the estimated COP and the real COP calculated with the help of the different approaches or given by the gathered operating points, respectively. All examined approaches are evaluated individually. Therefore, important statistical indicators like the standard deviation (σ) and the coefficient of determination (R^2) are used. Additionally, the correlation between the real COP and the estimated COP as well as the distribution of residuals are illustrated and analyzed.

The development of the approaches starts with a theoretical approach based on the Carnot-COP. To increase the quality of regression, the development of the following approaches successively incorporates the results of the evaluations of the previous.

Finally, a recommendation for one of the derived approaches is made (see Section 4.1.4). Therefore, the results from the individual evaluations as well as the trends of the estimated COP and the trend of η_{2nd} derived from the estimated COP are illustrated and compared. In addition, for a plausibility check, these trends are compared to the literature as well as to the expected trend based on a statistical evaluation of the gathered operating points. In Sections 4.2 and 4.3, the previously presented methodology of the regression analysis for SHPs and HTHPs is transferred to the other two derived HP-categories (VHTHPs and R717-HPs).

3.2 Economic and ecological evaluation

High accuracy of the COP estimation is a prerequisite for a reliable feasibility assessment of heat pump applications regarding their economic and ecological efficiency compared to conventional reference systems facing the knowledge gap on meaningful application possibilities of stakeholders, especially decision-makers. Heat pumps are often designed for stationary nominal operating conditions. Non-continuous process behavior can be smoothed by thermal energy storage. For this reason, the evaluation of an implementation based on the stationary COP at full load compared to the considerable effort of a dynamic simulation of a SCOP using software tools is an appropriate compromise. During the detailed planning phase, the SCOP is than to be estimated by the load and temperature profiles for each application individually.

To gain an impression of how important the accurate assessment of a COP is for the design and evaluation of economic and environmental efficiency compared to a reference system, and what other framework conditions influence the efficiency, a comparison is made based on a nomogram. A nomogram enables the approximate reading of key performance metrics through the graphic representation of mathematical functions.

3.2.1 Economic evaluation

Economic efficiency describes the ratio between profit and the effort required to achieve it. Wolf et al [30] provide a graphical orientation aid with a nomogram that shows the economic efficiency of a heat pump as a function of a constant η_{2nd}, ΔT_{lift} and final energy price ratio of electricity to natural gas c_{el}/c_{ng} compared to a common reference system, based on a standard gas boiler (SGB). Arpagaus [1] indicates the range of possible η_{2nd} between 0.4 and 0.6 with a typical value of 0.45, which is also confirmed by the results of this work, shown in Figure 11. The economic operation of heat pumps depends on $c_{el}/c_{ref,fu}$ and the reference system efficiency η_{ref} and is given for the fulfilment of Eq. 6-1 which is taken from Schlosser et al. [31]:

$$COP > max\left\{\frac{c_{el}}{c_{ref,fu}} \cdot \eta_{ref}\right\} \qquad \text{Eq. 3-1}$$

To make a sound investment decision between the two systems, investment ratios, depreciation period and interest-rate factor q must be considered. VDI 2067 [32] explains the calculation of LCOH of technical building equipment based on the annuity method. Annuity, A, contains capital-related costs (C_{cap}), operation-related costs (C_{op}) and demand-related costs (C_{dem}).

$$A_i = A_{C_{cap}} + A_{C_{op}} + A_{C_{dem}} = a \cdot [C_I + b_{op} \cdot f_{m,C} \cdot C_I + b_{dem} \cdot c_{fu} \cdot \frac{1}{\eta} \cdot \dot{Q}_{h,use} \cdot t_{oh}] \quad \text{Eq. 3-2}$$

The annuity factor combines one-off investment costs, C_I, and current payments and distributes the net present value of an investment with a calculation interest-rate factor q over the depreciation period N.

$$a = \frac{q-1}{1-q^{-N}} \quad \text{Eq. 3-3}$$

Here, price rises represented by the price dynamic cash value factor b_i is neglected due to the uncertainty of price inflation that is strongly influenced by both policy and economic climate. In this case, b_i is the inverse of a and the product a x b is equal to 1. The factor $f_{m,C}$ affects the C_{op} considering maintenance costs. C_{dem} for the yearly heat gain arises as a function of the final energy costs c_{fu} for a corresponding fuel and the efficiency η of the concerned conversion technology. The yearly heat demand is calculated by integrating a constant $\dot{Q}_{h,use}$ over the operating hours t_{oh}. The LCOH is the ratio of annuity to annual reference energy demand Q_{dem}.

$$LCOH_i = \frac{A_i}{Q_{dem}} \quad \text{Eq. 3-4}$$

To determine the cost parity ($LCOE_{HP} = LCOE_{ref}$) for a heat pump compared to a SGB, the $LCOH_{HP}$ and $LCOH_{SGB}$ are equated ($LCOE_{HP}/LCOE_{SGB,ng} = 1$) for the same heat demand over different c_{el}/c_{ng}. The nomogram displays cost ratios $LCOE_{HP}/LCOE_{SGB,ng}$ for different ΔT_{lift} and c_{el}/c_{ng}. ΔT_{lift} influences the COP regression function underlying the nomogram as η in Eq. 3-2. Since the standard deviation also records possible efficiencies below and above the regression the sensitive range (COP regression ± σ) must be specified for a sensitive assessment of possible economic viabilities.

3.2.2 Ecological evaluation

The ecological nomogram is based on the same principle, representing the ecological efficiency in terms of GHGE. GHGE correspond to the specific emissions of CO_2-equivalents (CO_2-e) per consumed quantity of final energy source. Within this framework, only energy-related GHGE during operation and not upstream and downstream emissions are taken into account. The ecological feasibility depends on the ratio of emission factors (EF) $EF_{elgrid}/EF_{fu,ref}$ of the electricity grid and the reference system fuel.

$$COP > max\left\{\frac{EF_{el,grid}}{EF_{fu,ref}} \cdot \eta_{ref}\right\}. \quad \text{Eq. 3-5}$$

Since the EF_{ng}, as the reference fuel used in this case, is physically constant the nomogram displays the cost ratio $GHGE_{HP}/GHGE_{SGB,ng}$ for different ΔT_{lift} and $EF_{el,grid}$. Analogous to 3.2.1, the COP function is specified in its sensitivity range.

4. Heat pump model development through regression analysis

Section 4.1 presents a detailed regression analysis to mathematical model the correlation between the COP and the operating conditions of SHPs & HTHPs with HFC and/or HFO. Sections 4.2 and 4.3 are building upon this and transferring the derived models to VHTHPs with HCFO, HFC or HFO as well as to SHPs and HTHPs with R717.

4.1 Standard and high temperature heat pumps with organic refrigerants

In the following different mathematical approaches to estimate the COP of a SHPs or HTHPs with organic refrigerants for any possible operation point within the given operation range are presented (see Sections 4.1.1 to 4.1.3), compared and a recommendation for one of these regressions is made (see Section 4.1.4).

4.1.1 Theoretical approach

The scope of this work covers subcritical HPs which use refrigerants without a temperature glide. The anticlockwise Carnot process is the comparison process for these HPs. According to the 2nd law of thermodynamics, the COP cannot exceed the Carnot-COP (see Eq. 4-1).

$$COP_{Carnot} = T_h/(T_h - T_l) \qquad \text{Eq. 4-1}$$

η_{2nd} compares the real COP of a HP and the Carnot-COP (see Eq. 4-2). In many feasibility assessments, the assumption is made that η_{2nd} is constant over the entire operating range. Depending on the type of HP, different values are given in the literature. For instance, van de Bor and Infante Ferreira [33] suggest 0.5 for industrial HPs in general. Wolf [34] recommends 0.45 to 0.50 for industrial water/water-HPs and 0.35 to 0.40 for industrial air/water-HPs. Arpagaus et. al. [12] recommend 0.45 for industrial water/water and water/steam HTHPs and VHTHPs.

$$\eta_{2nd} = COP/COP_{Carnot} \qquad \text{Eq. 4-2}$$

In practice, most heat sources and sinks provide or respectively use sensible heat. Thus, the heat source (T_l) and sink (T_h) temperatures are not constant when heat is transferred to or from the HP. In contrast to this, the Carnot process requires constant source and sink temperatures. To get closer to the Carnot process and achieve a high COP, ΔT_h and ΔT_l are usually chosen to be as small as practicable (see Sections 2.2.1 and 2.2.2). If this condition is met, ΔT_h and ΔT_l are usually ignored. Based on this, Eq. 4-3 can be used to estimate the COP.

$$COP = \eta_{2nd} \cdot T_{h,out}/(T_{h,out} - T_{l,in}) = \eta_{2nd} \cdot T_{h,out}/\Delta T_{lift} \qquad \text{Eq. 4-3}$$

The resulting η_{2nd} (see Table 5) from the regression analyses corresponds to the values from the literature listed above. Figure 10 (a) illustrates the quality of this approximation. With a perfect regression, all points would lie on the bisector between the estimated COP and the real COP and R^2 would be 1. In contrast to that, the real regression shows a variance and a localized bias. While for low COP the real value and estimation are almost equal with low variance, there is a notable negative bias for medium COP and a distinct positive bias for COP in the upper range.

Figure 10 (b) visualizes the distribution of the residuals. As the primary peak of the distribution lies in the negative values and a second peak in the positive residuals (> 0.95), the localized bias of the estimation is recognizable. Globally, the expected value (μ) is 0.00 and σ is 0.80.

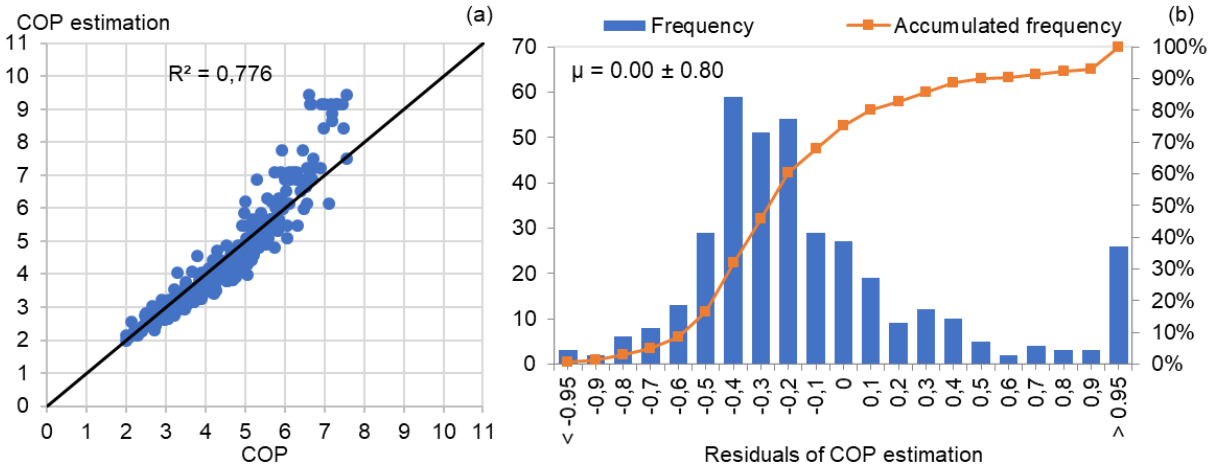

Figure 10: $COP = \eta_{2nd} \cdot T_{h,out}/\Delta T_{lift}$ - comparison of estimated COP and real COP (a) and frequency distribution of the residuals (b)

As shown above, the usage of a constant η_{2nd} for estimating the COP leads to a bias. As a result, η_{2nd} must be varying for operating conditions. To visualize this, Figure 11 presents a boxplot of η_{2nd} for ascending sorted categories of ΔT_{lift}. At first, η_{2nd} rises strongly, reaches its maximum at $35\ K \leq \Delta T_{lift} < 45\ K$ and then drops relatively weakly down again. The median of η_{2nd} ranges for the depicted ΔT_{lift}-categories from 0.25 to 0.49. Consequentially, the assumption of a constant η_{2nd} is only conditionally suitable for the COP-estimation.The trend which is discernible in Figure 11 strongly reminds to Figure 4 (d). As $\varepsilon_{isentropic}$ is a major influence on the COP and p_c/p_0 is strongly correlated to ΔT_{lift}, it is logical that these trends have a similar appearance.

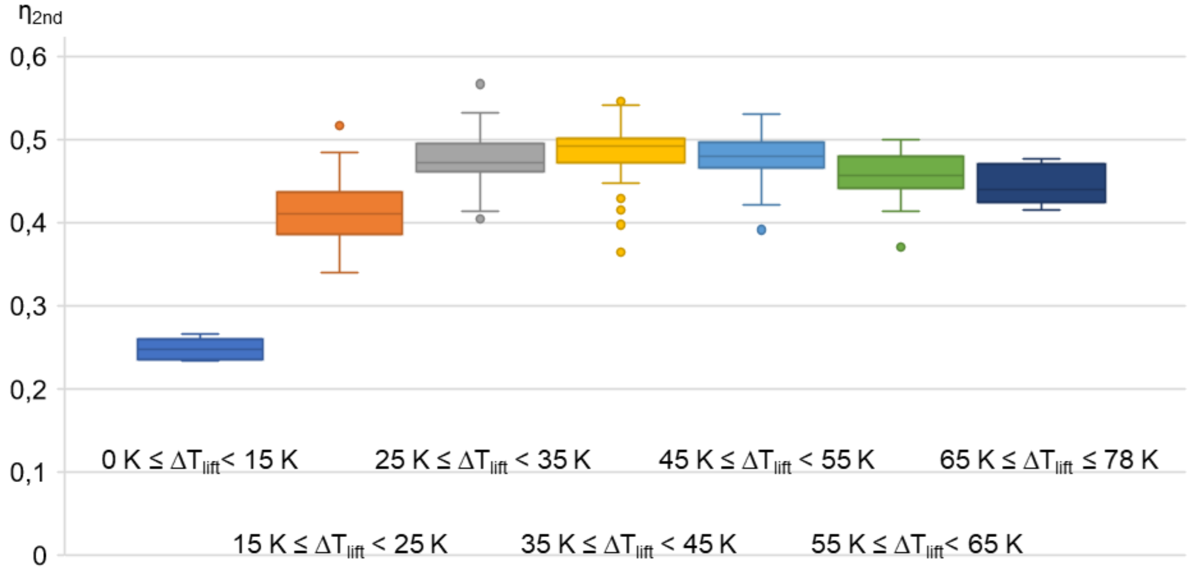

Figure 11: Boxplot of η_{2nd} for classified ΔT_{lift}

4.1.2 Semi-empirical extensions of the theoretical approach

Second law efficiency, η_{2nd}, includes all efficiency losses of a HP which occur in a certain operating point. The largest share of losses can be attributed to one of the following causes [33,35]:

- Compressor efficiency
- Heat losses to the environment
- Pressure drop
- Superheating
- Temperature driving forces at heat exchangers (condenser/ evaporator)
- Throttling losses

As already mentioned, the Carnot process is based on constant source and sink temperatures. Furthermore, the Carnot process ignores temperature difference between T_h and T_c as well as between T_l and T_0. To consider that the difference between T_0 and T_c is larger than ΔT_{lift}, Eq. 4-3 can be extended by a constant factor T_{dr} (see Eq. 4-4). To reduce the number of fit-parameters and to prevent overfitting, T_{dr} is assumed to be equal for condenser and evaporator. However, other influences like superheating or subcooling which may enlarge the difference between T_h and T_c or T_l and T_0 cannot be excluded when T_{dr} is fitted. According to the VDMA 24247-2 guideline [35], η_{KC} is intended to include all further loss mechanisms besides the temperature driving forces.

$$COP = \eta_{KC} \cdot (T_{h,out} + T_{dr})/(\Delta T_{lift} + 2 \cdot T_{dr}) \quad \text{Eq. 4-4}$$

Figure 12 visualizes the quality of the regression of Eq. 4-4 to the operating points. In comparison to Eq. 4-3 (see Table 5) σ has almost been halved and R^2 was significantly increased from 0.78 to 0.89. Still, the same pattern of locally occurring bias is recognizable: Low COP values are slightly overestimated, medium COP are underestimated and COP values in the upper range are strongly overestimated (see Figure 10).

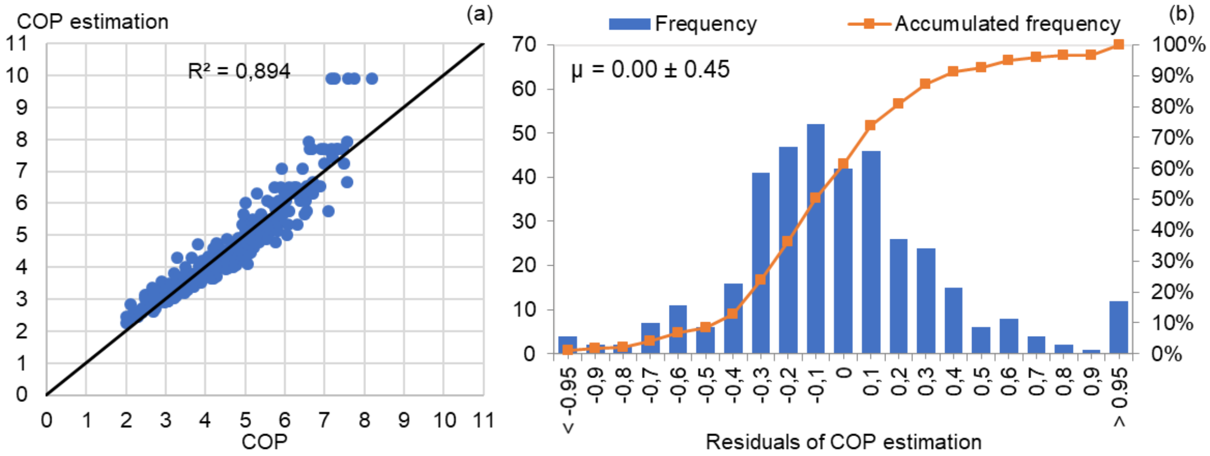

Figure 12: $COP = \eta_{KC} \cdot (T_{h,out} + T_{dr})/(\Delta T_{lift} + 2 \cdot T_{dr})$ - comparison of estimated COP and real COP (a) and frequency distribution of the residuals (b)

Eq. 4-5 provides a further extension of Eq. 4-3. By adding an exponent to both, the two main influencing variables of the Carnot-COP, ΔT_{lift} and $T_{h,out}$, can be weighted differently.

$$COP = a \cdot \Delta T_{lift}{}^{b} \cdot T_{h,out}{}^{c} \qquad \text{Eq. 4-5}$$

When fitting Eq. 4-5 to the operating points, R^2 and σ are slightly poorer in comparison to Eq. 4-4. Additionally, the same pattern of localized bias occurs (see Figure 13 (a)). However, besides a few extreme outliers in the upper COP range, the general deviation appears to be smaller. The outliers all result for operating points with a ΔT_{lift} of 10 K and overestimate the COP by more than two. When these outliers are ignored, a nearly normal distribution of residuals is recognizable around a residual of zero, as shown in Figure 13 (b).

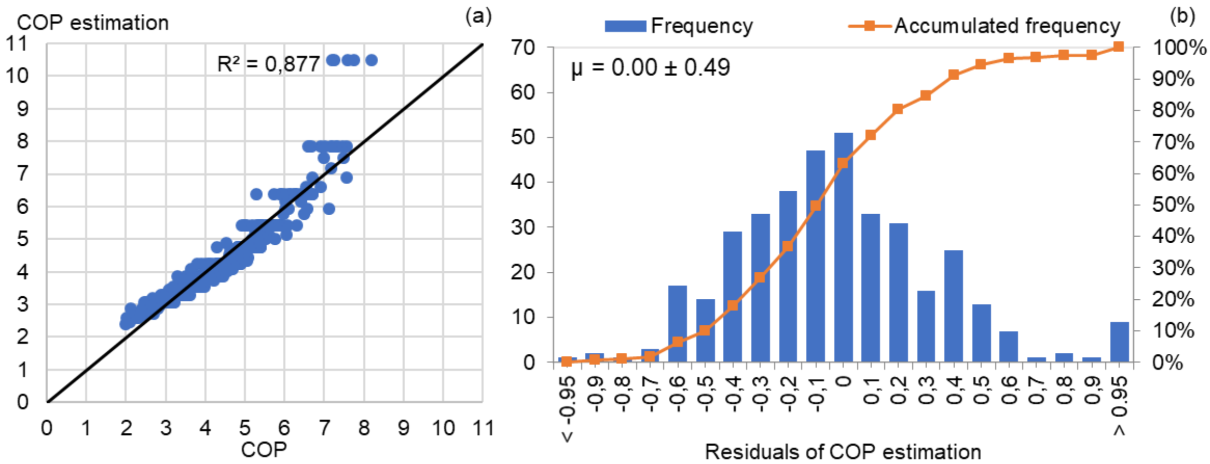

Figure 13: $COP = a \cdot \Delta T_{lift}{}^{b} \cdot T_{h,out}{}^{c}$ - comparison of estimated COP and real COP (a) and frequency distribution of the residuals (b)

The regression parameter c is fitted with 0.01, which means that the absolute temperature does not affect the COP. To further simplify Eq 4-5, a second fit with a given c = 0 was done. All parameters describing the quality of regression are almost similar for both fits. Differences can be identified at the fourth significant digit. For this work, only the second fit (c = 0) is presented (see Table 5).

The fact that the absolute temperature has practically no influence on the COP of real HPs stands in sharp contrast to the theoretical approach based on the Carnot-COP, what is illustrated in Figure 14. While the result of Eq. 4-3 ($\eta_{2nd} \cdot COP_{Carnot}$) rises for all ΔT_{lift} and especially for low ΔT_{lift}, the trends of the real COP are almost constant when $t_{h,out}$ is rising. A possible way to explain this behavior is presented below:

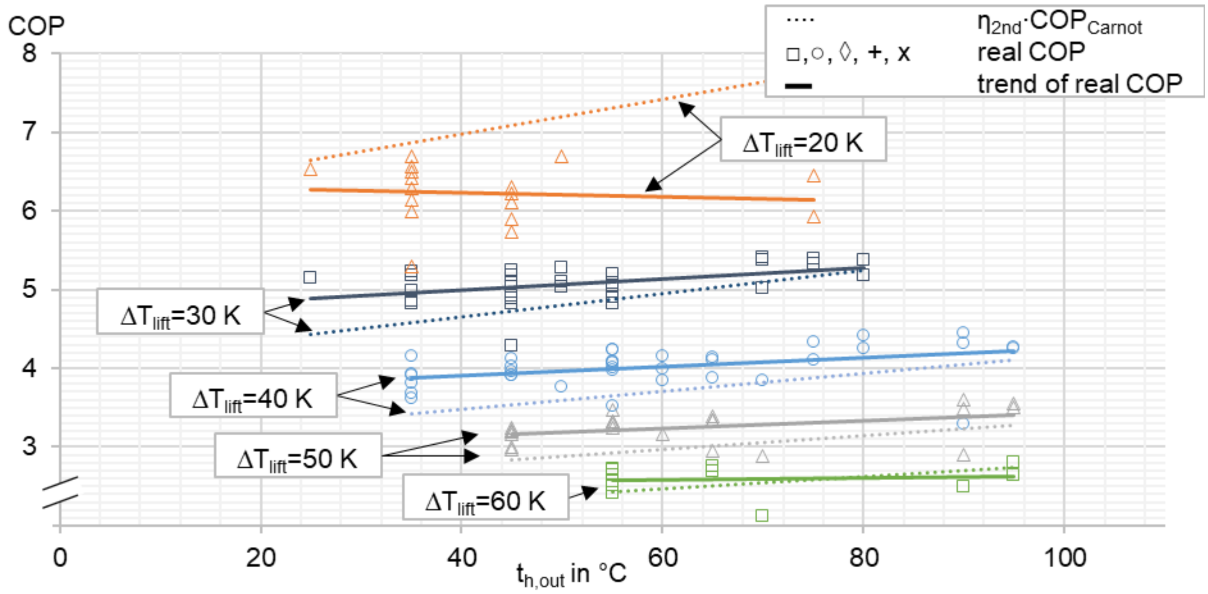

Figure 14: Comparison of the theoretical and practical influence of the absolute temperature on the COP for constant ΔT_{lift}. Notes: the dotted lines is Eq. 4-3 with η_{2nd}=0.45; straight lines are the linear trend of the several groups of operating points with constant ΔT_{lift}; and, to improve the clarity only a selection of data is shown.

Although the absolute deviation of the real COP between the individual HPs is low, it is quite high in comparison to the theoretical rise of the COP. Therefore, the theoretical increase of the COP, if it does occur for individual heat pumps, is difficult to detect. Furthermore, the COP of real HPs is influenced by various refrigerant properties. Many of these properties are affected by the absolute temperature. For instance, the absolute pressure, pressure ratio, heat capacity ratio, density and volumetric heating capacity are to be named. The resulting correlation between the COP and the absolute temperature for a constant ΔT_{lift} is schematically illustrated in Figure 4 (a). HPs are usually operated close to the COP peak if possible. On the left side of this optimum, an increase of the absolute temperature leads to a higher COP, which then peaks and begins to decrease with further absolute temperature increments. The relationship between absolute temperature and COP for a fixed ΔT_{lift} is a characteristic of the refrigerant, such that different refrigerants peak at different temperatures. The different temperature-COP relationships make it difficult to develop a single correlation for all refrigerants and all underlying operating points.

Eq. 4-6.1 combines the approaches of Eq. 4-4 and Eq. 4-5 into one equation. According to Eq. 4-5, c is set to zero without a significant loss of accuracy and b is limited to $-1 \leq b \leq 1$. Without this limit, the regression parameters are fitted with values that are not physically reasonable (see Eq. 4-6.2 in Table 5), which does not follow the semi-empirical approach. Nevertheless, when comparing the values of T_{dr} for Eq. 4-4 and Eq. 4-5 (see Table 5) major differences occur. Therefore, it must be assumed that the value of T_{dr} is mainly influenced by the respective mathematical equation and should not be physically interpreted or used for any kind of technical conclusion.

$$COP = a \cdot (\Delta T_{lift} + 2 \cdot T_{dr})^{b} \cdot (T_{h,out} + T_{dr})^{c} \qquad \text{Eq. 4-6.1}$$

The quality of regression, which can be reached with Eq. 4-6.1, is the best so far. Still, a localized bias is visible in Figure 15 (a). Even if the operating points with very high COP (ΔT_{lift} = 10 K) are ignored, low and high COP values are overestimated and medium COPs are underestimated. The same applies to the distribution of the residuals (see Figure 15 (b)). Although the residuals are almost normally distributed, the main peak is shifted to negative values and a second peak is visible for very high positive residuals (> 0.95), which results from the operating points with ΔT_{lift} = 10 K.

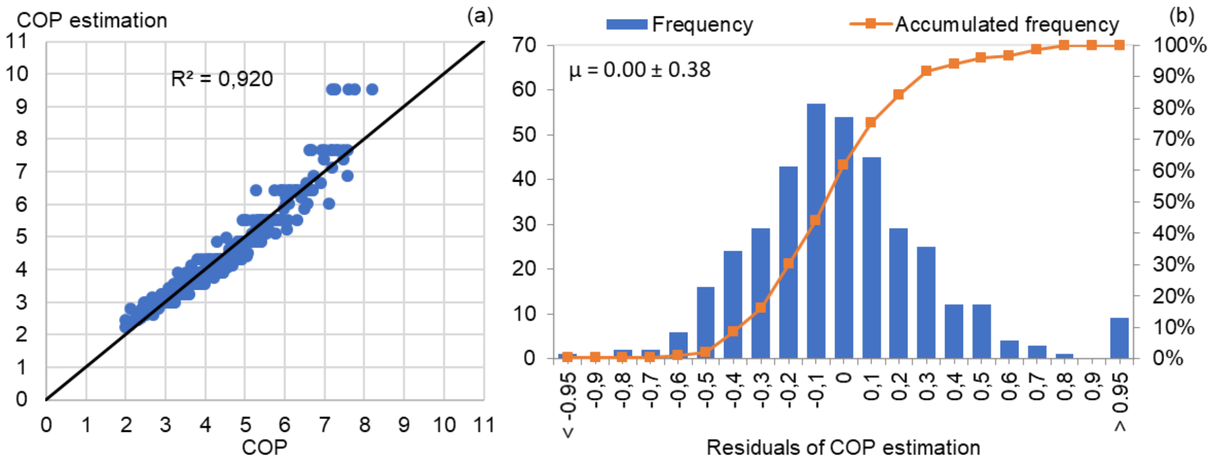

Figure 15: $COP = a \cdot (\Delta T_{lift} + 2 \cdot T_{dr})^b \cdot (T_{h,out} + T_{dr})^c$ – a comparison of estimated COP and real COP (a) and frequency distribution of the residuals (b).

4.1.3 Empirical approaches

As the theoretical and semi-empirical approaches struggle to adequately model the correlation between the operating temperatures and the COP without a bias, new empirical approaches are developed in this section. In the first step, the limitation of the exponents of Eq. 4-6.1 is removed. In doing so, the fitting parameters are not physically representative anymore and are renamed (see Eq. 4-6.2). Additionally, and similar to Eq. 4-5 and 4-6.1, the exponent of the second brackets (d) of Eq. 4-6.2 is set to zero without a significant loss of accuracy.

$$COP = a \cdot (\Delta T_{lift} + b)^c \cdot (T_{h,out} + 2 \cdot b)^d \qquad \text{Eq. 4-6.2}$$

The removal of the limitation of the fit parameter c leads to significant improvement in the quality of regression in comparison to all previous approaches. The bias of the estimation almost completely disappears (Figure 16). Only the very high COP for operating points with ΔT_{lift} = 10 K tend to continue to be overestimated. However, the overestimation of the COP of these operating points is significantly reduced but is still > 0.95 for some of these points. The substantially increased quality of regression is also underlined by the improved R^2 and σ (Table 5).

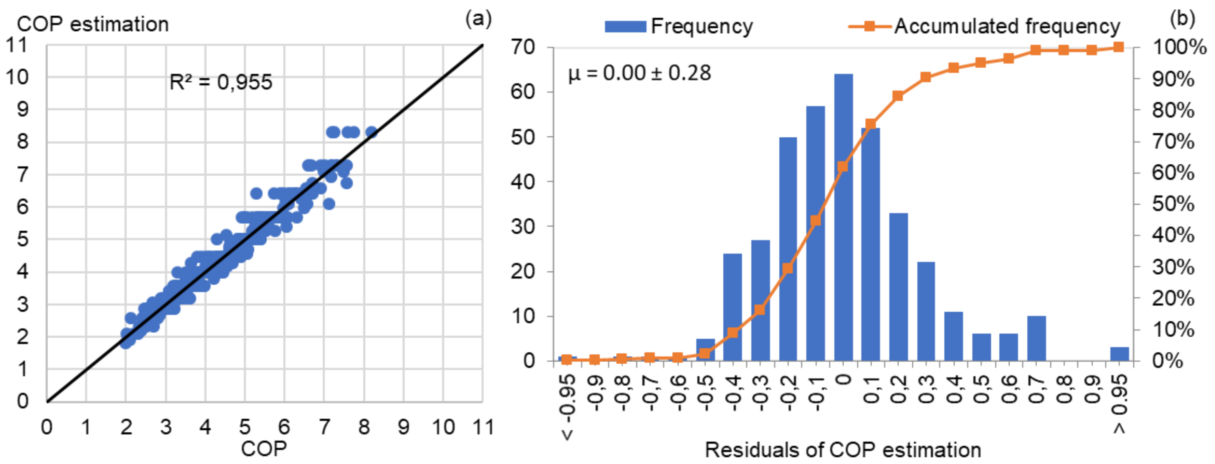

Figure 16: $COP = a \cdot (\Delta T_{lift} + 2 \cdot b)^c \cdot (T_{h,out} + b)^d$ – a comparison of estimated COP and real COP (a) and frequency distribution of the residuals (b).

Besides the power function (Eq. 4-6.2) that was derived from the semi-empirical approaches, several further empirical approaches were tested to see if a further increase in accuracy can be reached. The most promising of these are outlined in the following. As shown above, there is no significant correlation between $T_{h,out}$ and the COP within the examined HP category. Eq. 4-7 and Eq. 4-8 do not include a factor to consider the absolute temperature. Eq. 4-7 is an exponential function with the base e. The advantage of this equation is the small number of two fit parameters, which keeps the equation simple and prevents overfitting. Eq. 3.8 is a polynomial function of degree two. A polynomial of a higher degree is avoided to prevent an inflection point which would not fit the general trend of the COP (Figure 8 or Figure 9).

$$COP = a \cdot e^{b \cdot \Delta T_{lift}} \quad \text{Eq. 4-7}$$
$$COP = a \cdot \Delta T_{lift}{}^2 + b \cdot \Delta T_{lift} + c \quad \text{Eq. 4-8}$$

Both equations lead to a quality of regression almost identical to Eq. 4-6.2. This becomes visible by comparison of R^2 and σ (Table 5). Graphical illustrations of the quality of regression of Eq. 4-7 and Eq. 4-8 according to Figure 16 do not show any significant differences and are therefore not included in this work.

Table 5: Regression analysis for SHPs and HTHPs with HFC and HFO (all values are inserted unitless).

	#	Equation	μ	σ	R^2
Theoretical	4-3	$COP = \eta_{2nd} \cdot T_{h,out}/\Delta T_{lift}$ $\eta_{2nd} = 0.44532$	0.00	0.80	0.78
Semi-empirical	4-4	$COP = \eta_{KC} \cdot (T_{h,out} + T_{dr})/(\Delta T_{lift} + 2 \cdot T_{dr})$ $\eta_{KC} = 0.55441, T_{dr} = 3.7418$	0.00	0.45	0.89
	4-5	$COP = a \cdot \Delta T_{lift}{}^b \cdot T_{h,out}{}^c$ $a = 55.122, b = -0.72013, c = 0.0000$	0.00	0.49	0.88
	4-6.1	$COP = a \cdot (\Delta T_{lift} + 2 \cdot T_{dr})^b \cdot (T_{h,out} + T_{dr})^c$ $a = 197.78, b = -1.0000, c = 0.0000, T_{dr} = 5.3845$	0.00	0.38	0.92
Empirical	4-6.2*	$COP = a \cdot (\Delta T_{lift} + 2 \cdot b)^c \cdot (T_{h,out} + b)^d$ $a = 1.4480 \cdot 10^{12}, b = 88.730, c = -4.9460, d = 0.0000$	0.00	0.28	0.96
	4-7	$COP = a \cdot e^{b \cdot \Delta T_{lift}}$ $a = 10.204, b = -0.023347$	0.00	0.28	0.96
	4-8	$COP = a \cdot \Delta T^2 + b \cdot \Delta T + c$ $a = 0.0011651, b = -0.19041, c = 9.7522$	0.00	0.27	0.96
Range of validity	$-10\,°C \leq t_{l,in} < 60\,°C$ $25°C \leq t_{h,out} < 100\,°C$ $10K \leq \Delta T_{lift} \leq 78$ K				

* recommendation

4.1.4 Comparison and recommendation

The empirical approaches, in comparison to the semi-empirical and theoretical approaches, achieve significantly better R^2 and σ values (see Table 5). There are only marginal differences between the three empirical approaches. With the help of these approaches, the COP of a SHP or HTHP within the given temperature range can be estimated with a σ of less than 0.3 and an R^2 of 0.96.

Figure 17 visualizes the COP-estimation of all approaches presented in the previous. The standard deviations of the respective trends are not pictured but should be considered when the COP of a projected HP is estimated. The empirical approaches result in an almost linear trend that is slightly curved and fits the operating points well. In contrast to that, the theoretical and semi-empirical approaches result in a more strongly curved trend which causes the locally changing bias described in Sections 4.1.1 and 4.1.2.

Figure 18 visualizes the trend of η_{2nd} which is calculated for a constant $t_{h,out}$ of 60 °C. This figure illustrates the deviations between the different approaches, which are not visible in Figure 17 due to the scaling which is necessary to visualize the whole operating range. This is especially true when considering the upper end of the ΔT_{lift}-range where the maximum deviation between the approaches is 0.7 but the absolute COP is approximately 2.

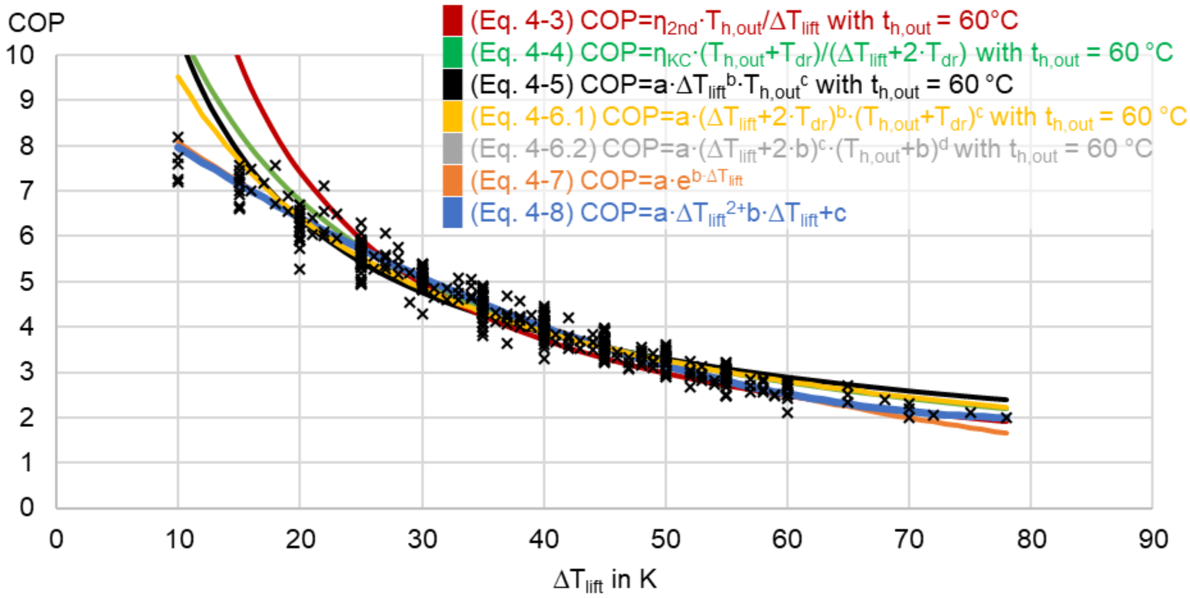

Figure 17: COP-estimation for different approaches. Notes: if the respective equation includes $t_{h,out}$, a value of $t_{h,out}$ = 60 °C is used; and, to keep the graph clear, the illustration of σ is omitted.

The theoretical and semi-empirical approaches lead to a constant or monotonically rising trend of η_{2nd}. This contradicts the previous finding that η_{2nd} has a maximum for medium ΔT_{lift} after which declines for further rising ΔT_{lift} (see Section 4.1.1). This underlines the conclusion that the theoretical and semi-empirical approaches are not appropriate for estimating the COP.

In contrast to the theoretical and semi-empirical approaches, the empirical approaches show a maximum of η_{2nd} for medium ΔT_{lift} and are in line with the expected trend derived from the literature and also the real trend which is visible in the boxplot of η_{2nd} (see Section 4.1.1.). For Eq. 4-8, a minimum occurs for a ΔT_{lift} of approximately 66 °C, which is not reasonable and suggests an overfitting of this equation. As a result, only the trends of Eq. 4-6.2 and Eq. 4-7 are fully plausible.

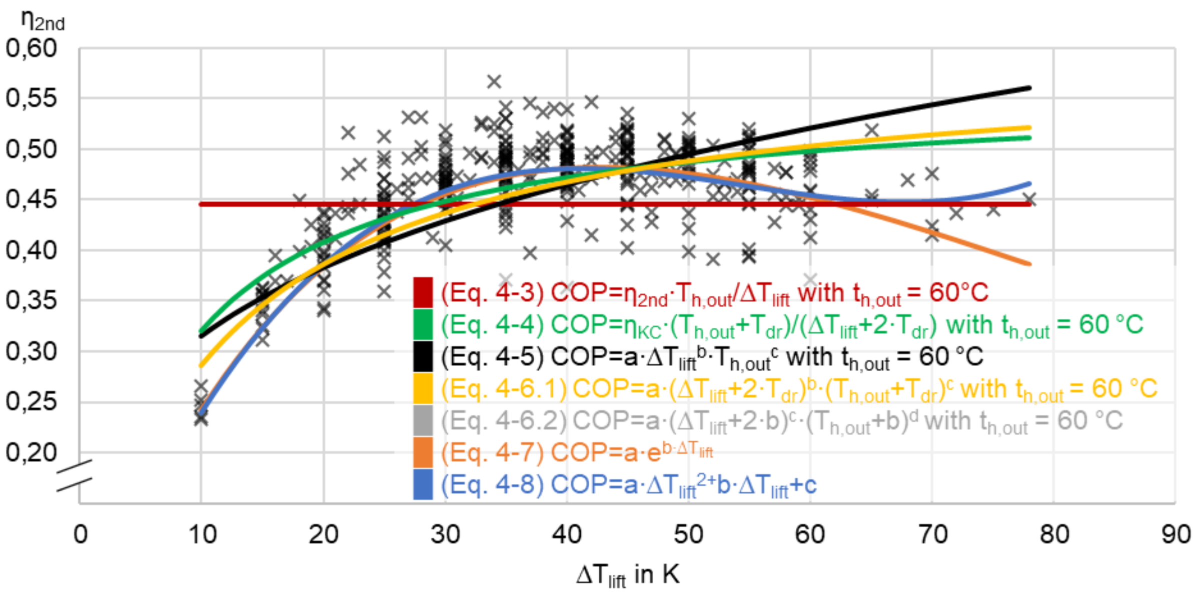

Figure 18: η_{2nd}-estimation for different approaches. Notes: $t_{h,out}$ = 60 °C is used for estimation of COP (if necessary) and COP_{Carnot}; and, to keep the graph clear, the illustration of σ is omitted.

When comparing all previous findings, Eq. 4-6.2 and Eq. 4-7 have little discernible difference. The trends of both equations are almost congruent for low and medium ΔT_{lift}, showing only a minor deviation in the upper range. As a result, both equations are appropriate for estimating the COP of SHPs and HTHPs with HFC and/or HFO which are represented in this section. When using this equation to fit another group of HPs, Eq. 4-6.2 could show advantages because it includes a factor to consider the influence of $t_{h,out}$. If fewer refrigerants or more similar refrigerants concerning the COP-optimum are used by the respective HPs, the influence of $t_{h,out}$ should be more relevant than was shown for the HPs covered in this section (see aslo Section 4.1.2).

4.2 Very high temperature heat pumps

In comparison to SHPs and HTHPs, the COP of the VHTHPs with organic refrigerants (HCFO, HFC or HFO) is on a similar level in the lower ΔT_{lift}-range and shows relative advantages in the upper ΔT_{lift}-range. Some of the VHTHPs covered in this work are designed to allow especially high single-staged ΔT_{lift} of up to 95 K. These HP use individually developed compressors which can handle higher absolute pressures and higher p_c/p_0 in comparison to the compressors operated in the remaining HPs (see Figure 4 (d)). The isentropic compressor efficiency optimum is also shifted to higher p_c/p_0, which explains why the COP of VHTHPs decreases less when ΔT_{lift} is increased. However, it must also be considered that the absolute operating temperatures of the VHTHPs are significantly higher in comparison to SHPs and HTHPs. Consequently, the fitted value of η_{2nd} of the VHTHPs is slightly lower in comparison to SHPs and HTHPs (η_{2nd} Table 6 and Table 7).

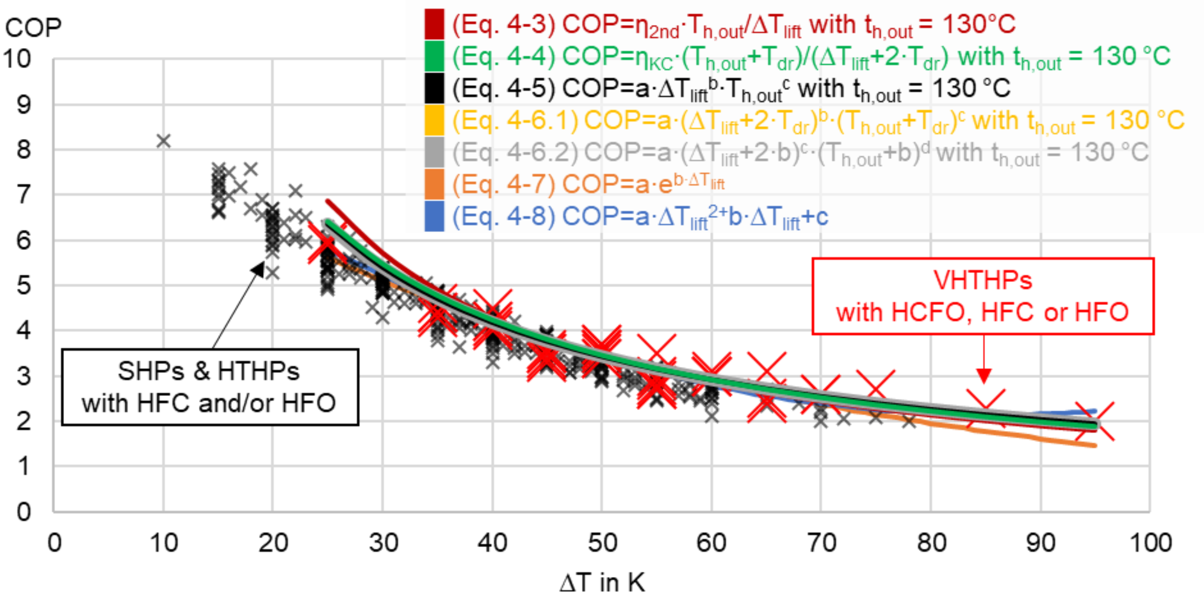

Figure 19: COP-estimation for different approaches. Notes: if the respective equation includes $t_{h,out}$, a value of $t_{h,out}$ = 130 °C is used; and, to keep the graph clear, the illustration of σ is omitted.

In contrast to the more diverse HP-category examined in Section 4.1, the influence of the absolute temperature on the COP is relevant for the HPs considered here. This is made clear by the fact that the parameter c in Eq. 4-5, 4-6.1 and 4-6.2 is fitted with a value not equal to zero (see Table 6). Additionally, Eq. 4-7 and Eq. 4-8, which do not include a factor to consider $t_{h,out}$, result in the least favorable quality of regression. This is probably because the refrigerants, which are covered here, have similar operating zones. As a result, the COP-characteristics of the refrigerants are more congruent and a correlation between the COP and the absolute temperature can be derived for this HP-category (compare to Section 4.1.2).

The trends of all approaches are almost congruent for VHTHPs (Figure 19). For the upper and lower end of the ΔT_{lift}-range, minor deviations between some of the approaches are visible which also cause minor differences in the quality of regression. Eq. 4-6.1 and Eq. 4-6.2 are completely identical fitted. Additionally, the trends and quality of regression of Eq. 4-4, Eq. 4-6.1 and Eq. 4-6.2 are completely identical. Therefore, these three approaches are recommended for the estimation of the COP for this HP-category and the given range of validity. However, it must be considered that the upper and lower ΔT_{lift}-range is crucial to show differences in the quality of regression (see Section 4.1), but only a few operating points below a ΔT_{lift} of 35 K and above of 65 K, while no operating points below a ΔT_{lift} of 25 K are covered. As a result, the validity of the regression analysis in the upper and lower ΔT_{lift}-range is low. If more operating points in the lower and upper ΔT_{lift}-range could be gathered, the assumption is reasonable that the COP-trend of these would be similar compared to SHPs and HTHPs, and Eq. 4-6.2 would be most advantageous.

Table 6: Regression analysis for VHTHPs with HCFO, HFC or HFO (all inserted values are unitless).

	#	Equation	μ	σ	R²
Theoretical	4-3	$COP = \eta_{2nd} \cdot T_{h,out}/\Delta T_{lift}$ $\eta_{2nd} = 0.42659$	0.00	0.22	0.94
Semi-empirical	4-4	$COP = \eta_{KC} \cdot (T_{h,out} + T_{dr})/(\Delta T_{lift} + 2 \cdot T_{dr})$ $\eta_{KC} = 0.46568, T_{dr} = 2.1966$	0.00	0.21	0.95
	4-5	$COP = a \cdot \Delta T_{lift}{}^{b} \cdot T_{h,out}{}^{c}$ $a = 1.8978, b = -0.88903, c = 0.67867$	0.00	0.19	0.95
	4-6.1*	$COP = a \cdot (\Delta T_{lift} + 2 \cdot T_{dr})^{b} \cdot (T_{h,out} + T_{dr})^{c}$ $a = 1.9118, b = -0.89094, c = 0.67895, T_{dr} = 0.044189$	0.00	0.19	0.95
Empirical	4-6.2	Eq. 4-6.1 = Eq. 4-6.2			
	4-7	$COP = a \cdot e^{b \cdot \Delta T_{lift}}$ $a = 9.0745, b = -0.0191512$	0.00	0.30	0.89
	4-8	$COP = a \cdot \Delta T^2 + b \cdot \Delta T + c$ $a = 9.9608 \cdot 10^{-4}, b = -0.17061, c = 9.4494$	0.00	0.27	0.91
Range of validity	$25\,°C \leq t_{l,in} \leq 110\,°C$ $80°C \leq t_{h,out} \leq 160\,°C$ $25K \leq \Delta T_{lift} \leq 95\,K$				

* recommendation

4.3 R717-heat pumps

This HP-category covers only 18 operating points from five different SHPs or HTHPs that use the natural refrigerant ammonia (R717). The range of validity and the validity of the regression analysis presented in the following are limited. Major differences of the COP of these HPs in comparison to HPs using HFC and/or HFO can be observed (Figure 20). The COP of most R717-operating points is clearly above of the COP of SHPs and HTHPs with HFC and/or HFO. But, as the operation of all R717-HPs covered in this work differs strongly from the rest of the HPs (see Section 2.2.2), no conclusion on a general advantage of this refrigerant in terms of efficiency can be drawn. Furthermore, the thermal output range of the covered R717-HPs is significantly larger than that of the rest of the HPs. As a result, the cost-benefit of R717-HPs, which results from scale effects, could lead to specifically larger designed components and what could be another reason for the relatively increased COP.

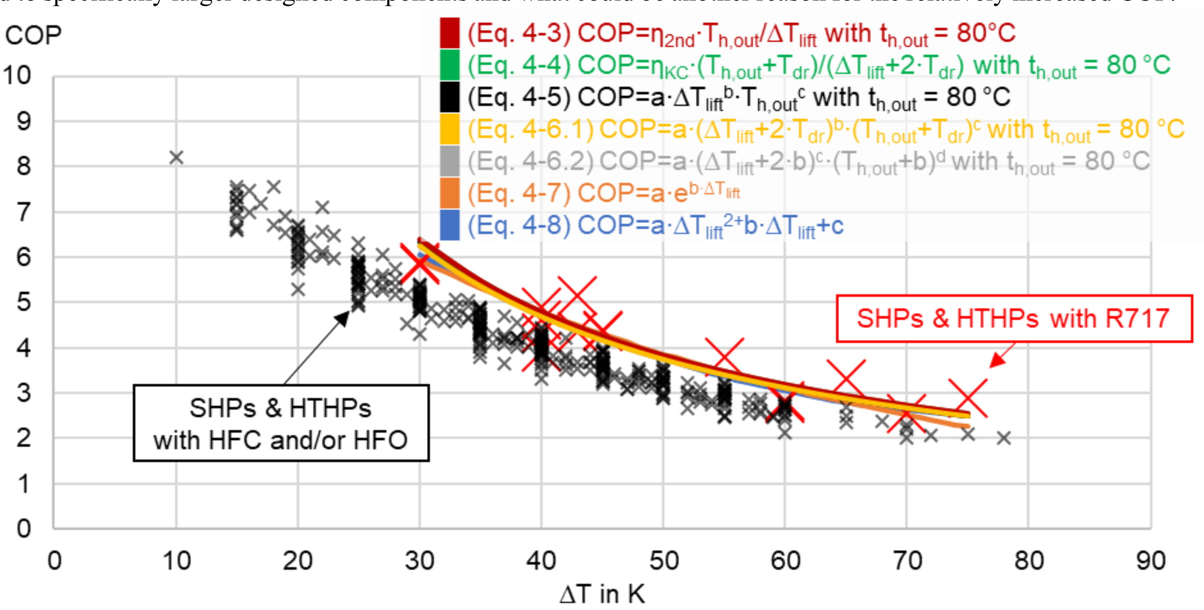

Figure 20: COP-estimation for different approaches. Notes: if the respective equation includes $t_{h,out}$, a value of $t_{h,out}$ = 80 °C is used; and, to keep the graph clear, the illustration of σ is omitted.

In contrast to the HPs examined in Section 4.1 and similar to the ones examined in Section 4.2, the influence of the absolute temperature on the COP is relevant for R717-HPs (see Table 7). The conclusion that this correlation becomes visible only for a group of HPs using refrigerants with similar COP characteristics is strengthened.

The trends of all approaches for estimating the COP of R717-HPs are almost congruent (Figure 20). Additionally, when comparing the quality of regression of these approaches, no significant difference is detectable (Table 7). This will probably be caused due to the low number of operating points. Moreover, as seen in Section 4.1 the largest absolute deviations between the different approaches appear within the ΔT_{lift}-range below 30 K. The fact that no operating points of R717-HPs in the lower ΔT_{lift}-range are covered in this work will additionally cause similar regression-quality of all approaches. Although no advantage of one approach for estimating the COP can be proved within this HP-category, Eq. 4-6.2 is recommended because it shows advantages in section 4.1 and 4.2.

Table 7: Regression analysis for SHPs & HTHPs with R717 (all inserted values are unitless).

	#	Equation	μ	σ	R^2
Theoretical	4-3	$COP = \eta_{2nd} \cdot T_{h,out}/\Delta T_{lift}$ $\eta_{2nd} = 0.54375$	0.00	0.41	0.87
Semi empirical	4-4	$COP = \eta_{KC} \cdot (T_{h,out} + T_{dr})/(\Delta T_{lift} + 2 \cdot T_{dr})$ $\eta_{KC} = 0.54375, T_{dr} = 0.0000$	0.00	0.41	0.87
	4-5	$COP = a \cdot \Delta {T_{lift}}^b \cdot {T_{h,out}}^c$ $a = 0.56989, b = -1.0168, c = 1.0000$	0.00	0.41	0.87
	4-6.1	$COP = a \cdot (\Delta T_{lift} + 2 \cdot T_{dr})^b \cdot (T_{h,out} + T_{dr})^c$ $a = 58.848, b = -1.0000, c = 0.19751, T_{dr} = 0.0000$	0.00	0.42	0.87
Empirical	4-6.2*	$COP = a \cdot (\Delta T_{lift} + 2 \cdot b)^c \cdot (T_{h,out} + b)^d$ $a = 40.789, b = 1.0305, c = -1.0489, d = 0.29998$	0.00	0.42	0.87
	4-7	$COP = a \cdot e^{b \cdot \Delta T_{lift}}$ $a = 11.314, b = -0.021488$	0.00	0.42	0.87
	4-8	$COP = a \cdot \Delta T^2 + b \cdot \Delta T + c$ $a = 0.0014515, b = -0.23104, c = 11.684$	0.00	0.41	0.88
Range of validity	$0\,°C \leq t_{l,in} \leq 40\,°C$ $70°C \leq t_{\mathrm{h,out}} \leq 85\,°C$ $30\mathrm{K} \leq \Delta \mathrm{T}_{lift} \leq 75\,\mathrm{K}$				

* recommendation

5. Economic and ecological evaluation

The recommended mathematical model Eq. 4-6.2 is used for comparison of LCOH and GHGE for different operating conditions at cost parity of HP and a conventional reference system represented by a SGB. As Eq. 4-6.2 is independent of the absolute sink temperature, the nomogram (see Figure 21) is valid for the whole range of validity of SHPs and HTHPs with HFC and/or HFO (see Table 5). The lines illustrating the standard deviation (Eq. 4-6.2 ± σ) record the possible range of variation. This can be used in terms of a sensitive assessment of possible economic and ecological viabilities.

Since 60 °C is in the middle of the validity range, it is selected as the sink temperature for calculating the 2nd law efficiency curves for constant η_{2nd}. To demonstrate the influence of η_{2nd}, the parity curves based on 2nd law efficiencies of 0.3, 0.45 and 0.6 are delineated.

5.1 Economic evaluation

Figure 21 illustrates ratios $LCOE_{HP}/LCOE_{SGB,ng}$ based on 3-2 to 3-4 and depending on different ΔT_{lift} and c_{el}/c_{ng}. The model parameters are summarized in Table 8:

Table 8: Selected nomogram parameters.

Parameter	SHP	SGB	Reference
C_I (incl. integration; without planning)	420 €/kW_{th} (300 kW)	60 €/kW_{th} (300 kW)	[34]
Operating hours t_{oh}	3500 h/y		[9]
Interest-rate factor q	1.07		[32,36]
Depreciation period N	20 y		[32,36]
Maintenance factor $f_{m,C}$	1.5 %		[32,36]
Full load efficiency η_{100}	COP (ΔT_{lift})	0.96 (300 kW)	Eq. 4-6-2 [32,36]

Not surprisingly, the localized bias of Eq. 4-3 (see section 4.1) is also reflected in Figure 21. While the mean 2nd law efficiency parity curve (η_{2nd} = 0.45) underestimates the economic efficiency in the range of 30 to 65 K, it overestimates the regression parity curve (4-6.2) for small (<30 K) and larger (>65 K) ΔT_{lift}.

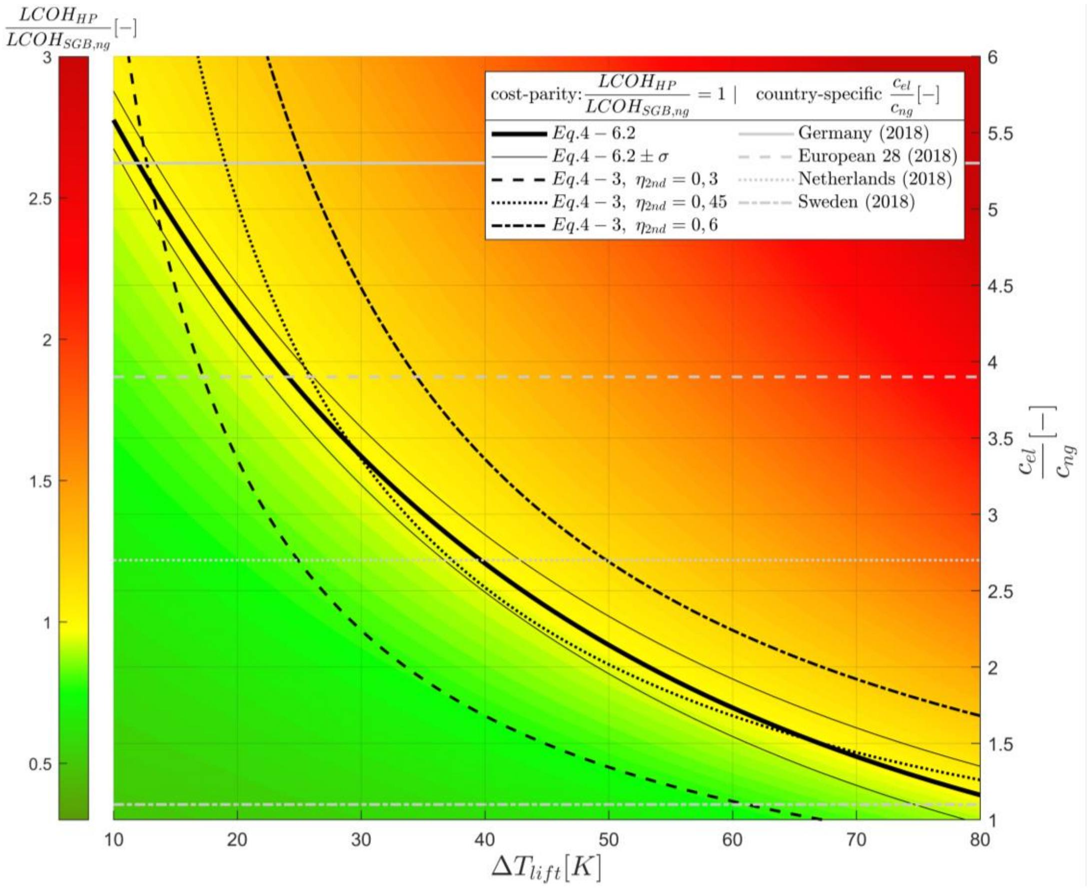

Figure 21: Nomogram of cost parity between SHP or HTHP and SGB for different ΔT_{lift} and $c_{el}/c_{ref.}$.

The price ratio has a major impact on profitability. The grey-dotted lines represent country-specific price ratios for the second half of 2018 considering all taxes and levies for consumption of electricity between 500 and 2000 MWh and of natural gas between 2778 MWh and 27,780 MWh. For non-electricity-intensive industrial companies in Germany (c_{el}/c_{ng} = 5.3), only implementations below a ΔT_{lift} of 15 K are economically recommended. The European average price ratio is 3.9:1, which allows economic integration concepts for ΔT_{lift} up to 25 K. In the Netherlands (2.7:1), Austria (3:1) or France (2.3:1), economical HP integration is possible up to a ΔT_{lift} of approximately 40 K. In Sweden (1.1:1), almost the whole technically ΔT_{lift} range is economically suitable [37].

Unfortunately, a two-dimensional nomogram represents only a small selection of general conditions. Besides the COP and the price ratio, the depreciation period, interest rate, investment costs and especially the operating hours influence the economic efficiency [1].

5.2 Ecological evaluation

In Figure 22, the GHGE of SGB and HP are compared using the developed method for COP estimation or respectively a constant full load efficiency (Table 8). The average German $EF_{el,grid}$ electricity mix is 474 gCO_2-e/kWh in 2018 and EF_{ng} is approximated by constant 202 gCO_2-e/kWh [38]. Additionally, a possible future value of $EF_{el,grid}$ is depicted by considering the climate protection scenario 95 (CPS95) that involves the reduction of GHGE by 95 % till 2050 compared to 1990 [39,40].

Already in 2018, a ΔT_{lift} of up to 60 K is ecologically reasonable in Germany. Based on the depicted scenario of a progressive decarbonisation of electricity, all future SHP or HTHP projects will be ecologically advantageous compared to the SGB by 2030 at the latest.

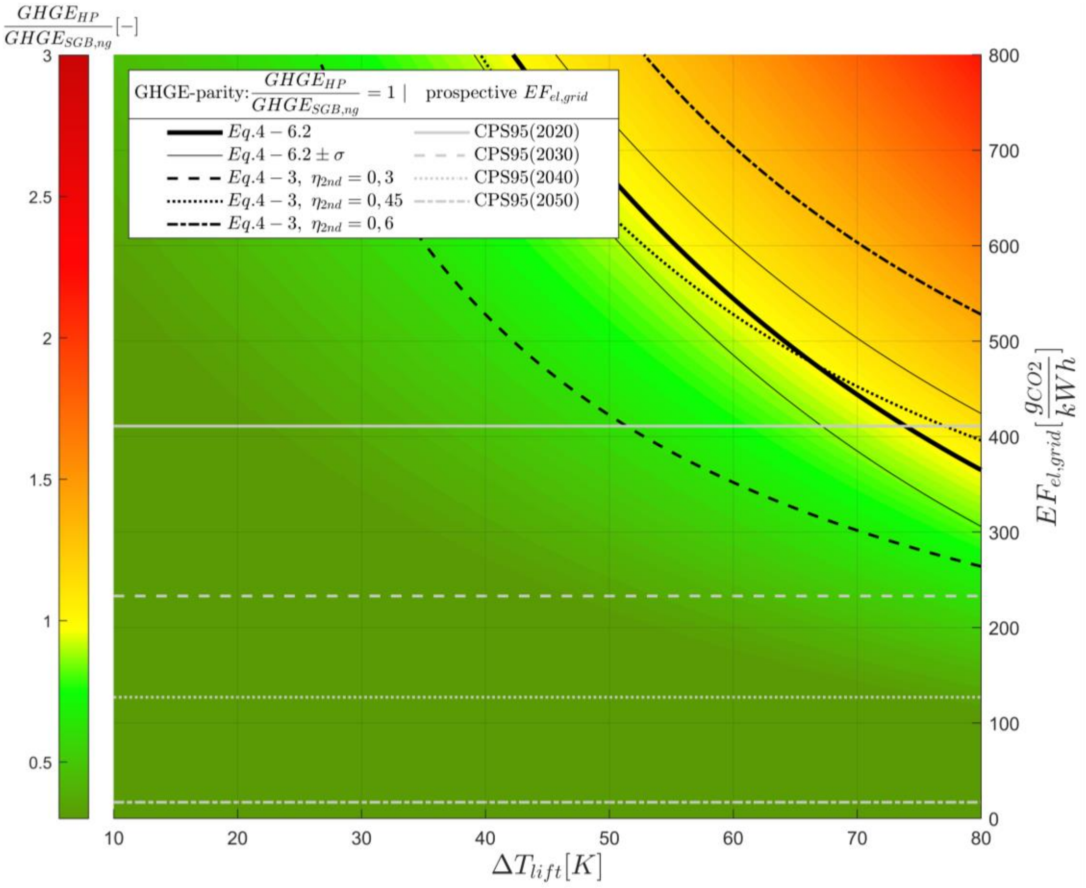

Figure 22: Nomogram of GHGE parity between SHP or HTHP and SGB for different ΔT_{lift} and $EF_{el,grid}$.

6. Conclusion

Large-scale HPs (> 50 kW_{th}) are an essential technology for the decarbonisation of the heat supply of industry, commerce and DH. Nevertheless, an information deficit on the capabilities of this technology is existing amongst important practitioners like energy-managers, and -consultants. To close this knowledge Gap, the capabilities of market available HPs are assessed within this work based on a comprehensive HP database. Especially for heat sink temperatures of up to 100 °C, the variety of available heat pumps from various manufacturers is particularly large. In this range, the offered HPs are covering a heat output from 50 kW_{th} up to several 1 MWth and the options of different system configurations, for instance concerning the usage of low GWP refrigerants, are versatile. Still, HPs using HFC with a relatively high GWP like R134a dominate the HP-market. HPs designed for heat sink temperatures of more than 100 °C up to 160 °C are less frequently offered but are also available. Regarding differences of the COP-characteristics of the evaluated HPs, a categorization concerning the designated range of $T_{h,out}$ and ΔT_h, which is depending on the refrigerant type (synthetic-organic or natural), is reasonable. A further characterization using criteria like compressor type or the specific refrigerant within the respective refrigerant-class does not reveal any significant differences of the COP characteristics.

The correlation between the efficiency and the operating conditions of market available HPs is also a crucial point, for which usually insufficient information is available among practitioners. The efficiency of a HP is usually published by manufactures by specifying the COP at a nominal operating point. Since in most cases the real operating conditions deviate from the published nominal operating point, the COP is usually estimated based on the Carnot-COP and η_{2nd}. Depending on the heat source and sink medium, η_{2nd}-values ranging from 0.35 to 0.6 can be found in literature and are assumed to be constant over the whole operating range. In contrast to that, the evaluation of the assembled database reveals that η_{2nd} is not constant as it is ranging from roughly 0.25 to 0.5 depending on ΔT_{lift}, even though only water as the heat source and sink medium is covered. Within the regression analysis, the correlation of the operating conditions and the COP of a HP was modelled. As R^2 is increased from 0.78 to 0.96 and σ is reduced from 0.80 to 0.28, the newly developed model is significantly more accurate and additionally eliminates a bias which is occurring when the COP is estimated based on Carnot-COP and a constant η_{2nd}. This bias leads to the fact that the economic and ecologically reasonability of HP projects is strongly overestimated for ΔT_{lift} in the lower range of up to 30 K, underestimated in the medium range from 30 to 65 K and overestimated in the upper range above of 65 K.

Within the economic evaluation, the importance of the electricity to gas price ratio is underlined as the main parameter that determines the economic suitability of a HP project. Whilst under German conditions ($c_{el}/c_{ng} = 5.3$), a SHP or HTHP project is scarcely economical at present, almost every SHP or HTHP project will be economically feasible in Sweden ($c_{el}/c_{ng} = 1.1$). In strong contrast to economics, the ecological evaluation finds that almost every SHP or HTHP project is already positive in Germany. Considering the progressive decarbonisation of electricity in the framework of the energy transition, the ecological advantage of future HP projects will become larger.

Acknowledgements

This work was supported by the German Federal Ministry for Economic Affairs and Energy within the framework of the 6th Energy Research Program [project: “SolarAutomotive”, grant number 0325863A]. The authors would like to thank all heat pump manufacturers for contributing to this work by providing data and additional information.

References

[1] Arpagaus C. High temperature heat pumps: Market overview, state of the art and potential applications. Berlin: VDE Verlag; 2019 (in German).

[2] Eder W, Moser F. The heat pump in process engineering. Vienna: Springer Vienna; 1979 (in German).

[3] Heat Pump & Thermal Storage Technology Center of Japan. Survey of Availability of Heat Pumps in the Food and Beverage Fields. Tokyo; 2010.

[4] Hita, A., Seck, G. Djemaa, A., Guerassimoff, G. Assessment of the potential of heat recovery in food and drink industry by the use of TIMES model. In: Lindström T, editor. Energy efficiency first: the foundation of a low-carbon society: ECEEE 2011 summer study ; conference proceedings ; 6 - 11 June 2011, Belambra Presqu'île de Giens, France. Stockholm: ECEEE; 2011, p. 735–743.

[5] Dupont, M., Sapora, E. The heat recovery potential in the French industry: which opportunities for heat pump systems? In: Broussous C, editor. Act! Innovate! Deliver!: Reducing energy demand sustainably ; ECEEE 2009 summer study ; conference proceedings ; 1 - 6 June 2009, La Colle sur Loup, France. Stockholm: ECEEE; 2009, p. 1115–1123.

[6] David A, Mathiesen BV, Averfalk H, Werner S, Lund H. Heat Roadmap Europe: Large-Scale Electric Heat Pumps in District Heating Systems. Energies 2017;10(4):578. https://doi.org/10.3390/en10040578.

[7] Paardekooper S, Lund RS, Mathiesen, B. V. et al. Heat Road Map Europe: Quantifying the Impact of Low-carbon Heating and Cooling Roadmaps. Copenhagen; 2018.

[8] Reckzügel, M., Meyer, M., Waldhoff, C., Ludwig, D., Tegeler, A., Schröder, I., Kebschull, O., Magnus, P., Niermann, U., Dering, N., Kruse, A., Vogel, K. Potential study industrial waste heat: LANUV-Fachbericht 96. Recklinghausen, Germany; 2019 (in German).

[9] Wolf S. Integration of heat pumps into industrial production systems: Potentials and instruments for tapping potential [Dissertation]. Stuttgart: Universität Stuttgart; 2017 (in German).

[10] Laue, H.J. et al. Application of Industrial Heat Pumps: Final Report - Part 2. Borås; 2014.

[11] Fleiter, T., Esland, R. Rehfeldt, M. et al. Heat Road Map Europe 2050, 2017. A low-carbon heating and cooling strategy: Deliverable 3.1: Profile of heating and cooling demand in 2015. Data annex. [October 21, 2019]; Available from: https://heatroadmap.eu/wp-content/uploads/2018/09/HRE4-Exchange-Template-WP3_v22b_website.xlsx.

[12] Arpagaus C, Bless F, Uhlmann M, Schiffmann J, Bertsch SS. High temperature heat pumps: Market overview, state of the art, research status, refrigerants, and application potentials. Energy 2018;152:985–1010. https://doi.org/10.1016/j.energy.2018.03.166.

[13] Lambauer J, Fahl U, Ohl M, Blesl M, Voß A. Industrial large-scale heat pumps: Potentials, barriers and best practice examples. Stuttgart; 2008 (in German).

[14] Laue, H.J. et al. Application of Industrial Heat Pumps: Final Report - Part 1; 2014.

[15] DIN German Institute for Standardization. Air conditioners, liquid chilling packages and heat pumps for space heating and cooling and process chillers, with electrically driven compressors - Part 1: Terms and definitions; German version EN 14511-1:2018. 2018th ed;01.040.27, 01.040.91, 27.080, 91.140.30(DIN EN 14511-1). Berlin, Germany: Beuth Verlag; 2019 (in German).

[16] DIN German Institute for Standardization. Air conditioners, liquid chilling packages and heat pumps for space heating and cooling and process chillers, with electrically driven compressors - Part 4: Requirements; German version EN 14511-4:2018. 2018th ed;27.080, 91.140.30(DIN EN 14511-4). Berlin: Beuth Verlag; 2019-07-00.

[17] DIN German Institute for Standardization. Air conditioners, liquid chilling packages and heat pumps for space heating and cooling and process chillers, with electrically driven compressors - Part 2: Test conditions; German version EN 14511-2:2018. 2018th ed;27.080, 91.140.30(DIN EN 14511-2). Berlin, Germany: Beuth Verlag; 2019 (in German).

[18] DIN German Institute for Standardization. Air conditioners, liquid chilling packages and heat pumps for space heating and cooling and process chillers, with electrically driven compressors - Part 3: Test methods; German version EN 14511-3:2018. 2018th ed;27.080, 91.140.30(DIN EN 14511-3). Berlin, Germany: Beuth Verlag; 2019 (in German).

[19] Association of German Engineers. Calculation of the seasonal coefficient of performance of heat pumps - Electric heat pumps for space heating and domestic hot water. 03th ed;27.080, 91.140.10(VDI 4650 Blatt 1). Berlin, Germany: Beuth Verlag; 2019.

[20] Schlosser F, Seevers J-P, Peesel R-H, Walmsley TG. System efficient integration of standby control and heat pump storage systems in manufacturing processes. Energy 2019;181:395–406. https://doi.org/10.1016/j.energy.2019.05.113.

[21] Jakobs, R., Laue,H.J. Application of industrial heat pumps IEA HPP IETS Annex 35-13 IEA HPC: Workshop regarding heat pumps and IEA projects. In: Application of Industrial Heat Pumps: Workshop reagarding heat pumps and IEA projects; 2015, p. 1–82.

[22] Peureux, J.-L., Sicard, F., Bobelin, D. French industrial heat pump developments applied to heat recovery. In: 11th IEA Heap Pump conference; 2014.

[23] Bobelin, D., Bourig, A., Peureux, J. Experimental results of a newly developed very high temperature industrial heat pump (140C) equipped with scroll compressors and working with a new blend refrigerant. In: International Rfrigeration and Air Conditioning Conference; 2012, p. 1–10.

[24] Peureux, J., Sapora, E., Bobelin, D. Very high-temperature heat pumps applied to energy efficiency in industry. In: ACHEMA; 2012.

[25] DIN German Institute for Standardization. Refrigerating systems and heat pumps - Safety and environmental requirements - Part 1: Basic requirements, definitions, classification and selection criteria; German version EN 378-1:2016. 2016th ed;01.040.27, 27.080, 27.200. Berlin, Germany: Beuth Verlag; 2018 (in German).

[26] PanGas. SAFETY DATA SHEET - R513A. Dagmersellen, Switzerland; 2018.

[27] ASHRAE. Standard 34 - Safety Standard for Refrigeration Systems and Designation and Classification of Refrigerants; 2016.

[28] Maurer T. Refrigeration technology for engineers. Berlin, Offenbach: VDE Verlag GmbH; 2016 (in German).

[29] VDI-Heat atlas. 11th ed. Berlin: Springer Vieweg; 2013 (in German).

[30] Wolf S, Flatau R, Radgen P, Blesl M. Systematic application of large-scale heat pumps in Swiss industry. Bern; 2017 (in German).

[31] Schlosser F, Arpagaus C, Walmsley TG. Heat Pump Integration by Pinch Analysis for Industrial Applications: A Review. CHEMICAL ENGINEERING TRANSACTIONS 2017;76:7–12. https://doi.org/10.3303/CET1976002.

[32] Association of German Engineers. Economic efficiency of building installations - Fundamentals and economic calculation. 09th ed;ICS 91.140.01(VDI 2067 Blatt 1). Berlin, Germany: Beuth Verlag; 2012.

[33] van de Bor DM, Infante Ferreira CA. Quick selection of industrial heat pump types including the impact of thermodynamic losses. Energy 2013;53:312–22. https://doi.org/10.1016/j.energy.2013.02.065.

[34] Wolf S, Fahl U, Blesl M, Voß A, Jakobs R. Analysis of the potential of industrial heat pumps in Germany. Endbericht. Stuttgart; 2014 (in German).

[35] Verband Deutscher Maschinen- und Anlagenbau e. V. Energy efficiency of refrigerating systems - Part 2: Requirements for system design and components;ICS 27.015; 27.200(VDMA 24247-2). Berlin, Germany: Beuth Verlag; 2018; Available from: https://www.vdma.org/documents/105628/22968062/Entwurf%20VDMA%2024247-2_2018-02_1513696466071.pdf/8d7786a1-83b0-42a7-aaea-e84d1b0beba3. [November 07, 2019].

[36] Association of German Engineers. Economic efficiency of building installations - Fundamentals and economic calculation. 12th ed;ICS 91.140.01(VDI 2067 Blatt 40). Berlin, Germany: Beuth Verlag; 2013.

[37] Eurostat. Electricity prices for non-household consumer. & Gas prices for non-household consumer. [December 10, 2019]; Available from: https://ec.europa.eu/eurostat/web/energy/data/database.

[38] Icha P, Kuhs G. Development of specific carbon dioxide emissions of the German electricity mix in the years 1990 - 2018. Dessau-Roßlau; 2019 (in German).

[39] Repenning J, Emele L, Blanck R, Böttcher H, Dehoust G, Förster Hea. Climate protection scenario 2050: 2nd final report. Berlin; 2015 (in German).

[40] Greiner B, Hermann H. Sectoral emission paths in Germany until 2050: Power generation. Berlin; 2016 (in German).